Computer experiments of vacuum injection of pellet beam via buffer gas flow

Victor. L. Varentsov*
Institute for Theoretical and Experimental Physics,
B. Cheremushkinskaya 25, 117218, Moscow, Russia

ABSTRACT

Operation of the Moscow-Jülich pellet-generator has been studied by means of computer experiments. For this purpose detailed gas dynamic simulations based on the solution of a full system of time-dependent Navier-Stokes equations have been performed for hydrogen buffer gas flow. The results of gas dynamic calculations were used then for detailed pellet trajectory simulations under the effect of the buffer gas flow. In series of additional computer experiments has been shown that a performance of the Moscow-Jülich pellet-generator can be easily improved by means of some changes of the 1st sluice geometry. So, e.g. it will allow reduce required pumping speed of vacuum pumps by factor of 3.65.

Keywords: Liquid hydrogen micro-droplets, pellet target, subsonic and supersonic buffer gas flow, computer simulation

1. INTRODUCTION

A high density internal hydrogen target is required for experiments at PANDA detector and two different internal targets are under development (see e.g. Ref. [1]). They are a cluster-jet target and a pellet target that consists of a beam of frozen micro-droplets of hydrogen.

Shortly, process of pellets generation can be briefly described in the following way. A thin liquid hydrogen jet is produced by pressing the cooled liquid hydrogen through a miniature converging nozzle into a chamber filled with a buffer gas. This liquid jet breaks-up into uniformly sized and spaced micro-droplets by means of acoustical excitation. Then the liquid hydrogen droplets are extracted into vacuum passing through a long thin separation capillary (or sluice) via the buffer gas flow. Behind the capillary exit the buffer gas expands into vacuum as a supersonic gas jet; the gas temperature, pressure and density in this gas jet drastically decrease and in result of liquid droplets surface evaporation they transform to frozen micro-spheres (called pellets). Downstream the separation capillary a skimmer (or 2nd sluice) is installed on the gas-jet axis. It serves as a pellet-beam collimator and permits to use of differential pumping to meet vacuum requirements in the storage ring.

Two main hydrogen pellet-generators have been developed. In the first one developed at Uppsala (e.g. Refs. [2, 3]) a buffer gas that consists of a helium-hydrogen mixture at low stagnation pressure P_o = 21 mbar (~13 mbar of helium and ~8 mbar of hydrogen) and stagnation temperature T_o = 14.1 K is used. The measured initial droplet velocity here V_{in} = 37.7 m/s that corresponds to estimated velocity of the liquid jet V_{jet} = 37.9 m/s. Second hydrogen pellet-generator that has been developed by joint Moscow-Jülich team [4] operates with a pure hydrogen buffer gas and at hither stagnation pressure and temperature.

Operation of the Moscow-Jülich pellet-generator I studied by means of computer experiments, which results I present in this report. First, I have performed detailed gas dynamic simulations of the hydrogen buffer gas flow: in the region between the nozzle and the 1st sluice exit there is a subsonic gas flow, but between the 1st and 2nd sluices the buffer gas expands into vacuum as a free supersonic gas-jet. The results of these gas dynamic calculations I used then for detailed pellet trajectory simulations.

I did not consider here the process of the liquid jet decay into droplets that occurs at relatively short distances from the nozzle exit.

*E-mail address: v.varentsov@gsi.de; phone +49 6159 71 16 38

2. GENERAL DISCRIPTION

2.1 Moscow-Jülich pellet-generator design

Description of the Moscow-Jülich pellet-generator design I have got by e-mail from A. Boukharov [5].

The converging nozzle produced from a glass tube has a length of 7 mm and an exit-hole diameter equal to 12 μm.

The 1st sluice consists of three following parts. First (entrance) part of the sluice is a cylindrical tube of 54 mm length, which inner diameter is 4 mm. It is installed on the axis at 16 mm distance downstream the nozzle exit.

The end of this tube joins by glue the second (transitional) sluice part of 15 mm length that also has a circular cross section with an inner diameter that decreases exponentially from 4 mm to 0.6 mm in the buffer gas flow direction.

The third (exit) part of this sluice is a glass tube of 81 mm length and of 0.6 mm in inner diameter attached to the end of the second one.

Therefore, total length of the sluice amounts to 150 mm.

The distance between 1st sluice exit and 2nd sluice entrance is 250 mm. I have no information about the 2nd sluice design, but it is unimportant here, because the 2nd sluice does not affect on the pellet-beam formation and works only as a beam collimator.

The described pellet-generator operates at the following conditions. The nozzle and 1st sluice temperature, as well as, a buffer gas stagnation temperature are equal to 20 K. Stagnation buffer gas pressure P_o = 100 mbar; ambient buffer gas pressure behind the 1st sluice $P_a = 6 \cdot 10^{-2}$ mbar. Background pressure behind the 2nd sluice is $1 \cdot 10^{-3}$ mbar.

Velocity of the liquid jet (before it breaks-up into micro-droplets) V_{jet} = 4 m/s, which length is in the range of 1÷5 mm. Unfortunately, I could not get from the Moscow-Jülich team any data about initial droplet-beam angular divergence after the liquid jet decay.

The hydrogen droplets have diameters ≥ 20 μm.

2.2 Gas dynamic simulations

Gas dynamic simulations of the buffer gas flow have been performed using our VARJET code. This code is based on the solution of a full system of time-dependent Navier-Stokes equations for multicomponent gas mixtures and is described in detail in Ref. [6]. It has been carefully checked and I have successfully used it for development of the LEBIT [7] (Michigan State University, East Lansing) and SHIPTRAP [8] (SGI, Darmstadt) projects for the buffer gas cooling of radioactive ion beams and for development of the ASACUSA gas-jet target [9] (CERN, Geneva), as well. Results and descriptions of the other our numerical investigations of the ion beam buffer gas cooling technique one can find in Refs. [10-12].

In the last year I finished VARJET calculations for R&D of a gas-target setup for matter and antimatter collisions with antiprotons and heavy highly charged ions at the HITRAP facility within the FAIR-Collaborations SPARS and FLAIR [13]. I used VARJET code also for development of a focused ion beam source of a new type for micro- and nanoelectronics technologies [14].

An influence of the liquid hydrogen jet and droplets on the buffer gas flow field parameters has been neglected, because the droplets (~ 20÷50 μm in diameter) occupy only a small fraction of a buffer gas flow cross section even in the narrowest part of the sluice (it is the glass tube with inner diameter of 600 μm).

2.3 Pellet trajectory simulations

Results of the gas dynamic calculations (flow fields of buffer gas density, temperature and velocity components) were incorporated in the other code [15] for detailed pellet trajectory simulations.

At operation conditions of the Moscow-Jülich pellet-generator the droplets (or/and pellets) sizes are much larger than mean free pass values of the hydrogen buffer gas molecules. Therefore, the droplet dynamics in the buffer gas flow can be described in framework of continuum theory, where droplet moves in the gas under action of a viscous drag force. In the region downstream the 1st sluice exit, where buffer gas density drastically decreases due to the supersonic gas jet expansion into vacuum, the continuum theory should be corrected.

An expression for the drag force $\mathbf{F}_D$ on a spherical particle (in our case it is a droplet or pellet) of radius $\mathbf{r_p}$ in a gas can be written as [16]:

$$F_D = -\frac{1}{2}\pi r_p^2 \rho_{gas} |V_{rel}| V_{rel} \frac{C_D}{C_C} \quad , \qquad (1)$$

where $\mathbf{V}_{rel} = \mathbf{V}_p - \mathbf{V}_{gas}$ is the relative velocity between the particle velocity $\mathbf{V}_p$ and the buffer gas velocity $\mathbf{V}_{gas}$, ρ_{gas} is the buffer gas density, C_D is the drag factor, which expression depends on the local Reynolds number for the particle in the buffer gas flow (see for details Ref. [16]), and C_C is Cunningham rarefaction correction that can be written as [16]:

$$C_C = 1 + \frac{\lambda_{gas}}{r_p}\left[1.257 + 0.4\exp\left(-1.1\, r_p/\lambda_{gas}\right)\right] \quad , \quad (2)$$

where λ_{gas} is a mean free pass of the hydrogen gas molecules.

Because of viscosity the buffer gas velocity distribution across the sluice channels has a parabolic shape with a maximum value on the axis (e.g. see Fig. 3 bellow, where results of gas dynamic calculations for radial gas velocity distribution in the middle of the third part of the sluice is shown). It means that the gas velocity on the side of the droplet towards the axis is higher than that one towards the channel wall. So, due to Bernoulli's low there is a force that compels the droplets move to the axis. This Bernoulli's force is proportional to the buffer gas density, the droplet cross section, the relative velocity $\mathbf{V}_{rel}$ and the difference of the gas velocities on the two sides of the droplet. This focusing effect of the buffer gas flow inside the sluice has been also taken into account in the pellet trajectory simulations.

3. CALCULATION RESULTS

3.1 Results of gas dynamic calculations

Some results of gas dynamic simulations for the Moscow-Jülich pellet-generator are presented in Figs. 1-10.

Results of calculation for the H_2 buffer gas velocity flow field in different parts of the sluice are shown in Figs. 1-4. The radial buffer gas velocity distribution in the middle of the 3rd part of the sluice is shown in the Fig. 3.

Figs. 5 and 6 are similar to Fig.4, but it show gas flow fields of temperature and density, correspondingly.

The buffer gas flow out the sluice into vacuum at ambient pressure $P_a = 6\cdot10^{-2}$ mbar via free supersonic gas-jet expansion. Details of this supersonic jet structure are shown in Figs. 7-9. There is a well-marked classic Mach disk at ~11 mm distance downstream the sluice exit. The buffer gas passing through this Mach disk undergoes a transition from supersonic regime to subsonic one. After that the gas accelerates up to supersonic velocities again.

Fig. 10 shows the H_2 buffer gas static pressure distribution along the axis. Notice that an ambient pressure in this vacuum chamber $P_a = 6\cdot10^{-2}$ mbar, which 300 times higher than the static pressure on the axis of supersonic jet upstream the Mach disk (e.g. at 10 mm distance from the sluice exit).

The hydrogen buffer gas flow rate through the 1st sluice $Q = 8.67\cdot10^{20}$ mol./s that corresponds to 36.1 mbar l/s at room temperature. So, to maintain $6\cdot10^{-2}$ mbar ambient pressure in the vacuum chamber between 1st and 2nd sluice it is necessary to use a vacuum pump of 602 l/s effective pumping speed. It can not be a compact turbo molecular pump

because of a bad vacuum for turbo molecular pumps operation. For pumping one need here to use a large Roots pump, which nominal pumping speed should be higher than 2200 m^3/h.

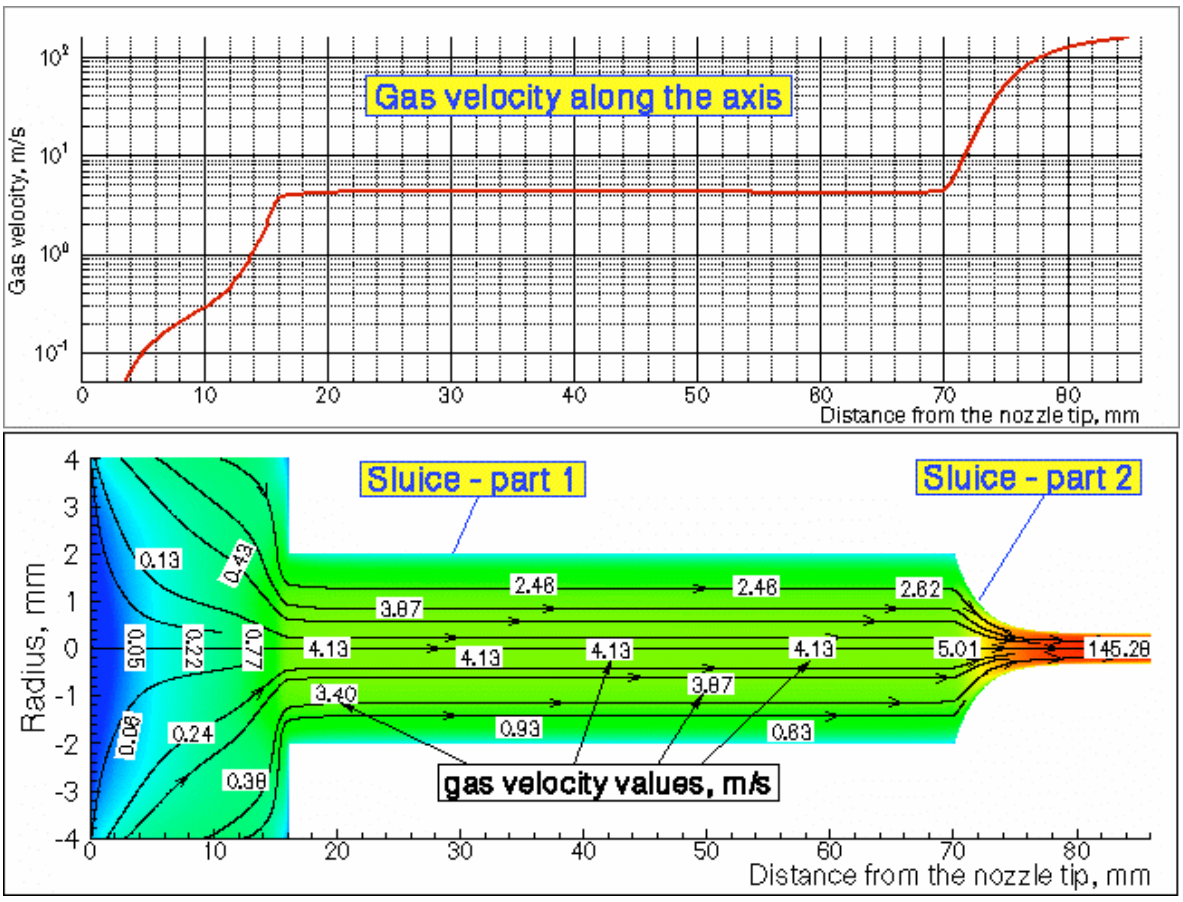

Fig.1. Colored plot of the H_2 buffer gas velocity flow field in the region from the nozzle exit to the sluice entrance and inside the first part of the sluice (bottom): black arrowhead lines are the H_2 gas streamlines; the red color represents maximum and the blue color – minimum velocity values. The gas velocity distribution along the axis is shown in the top.

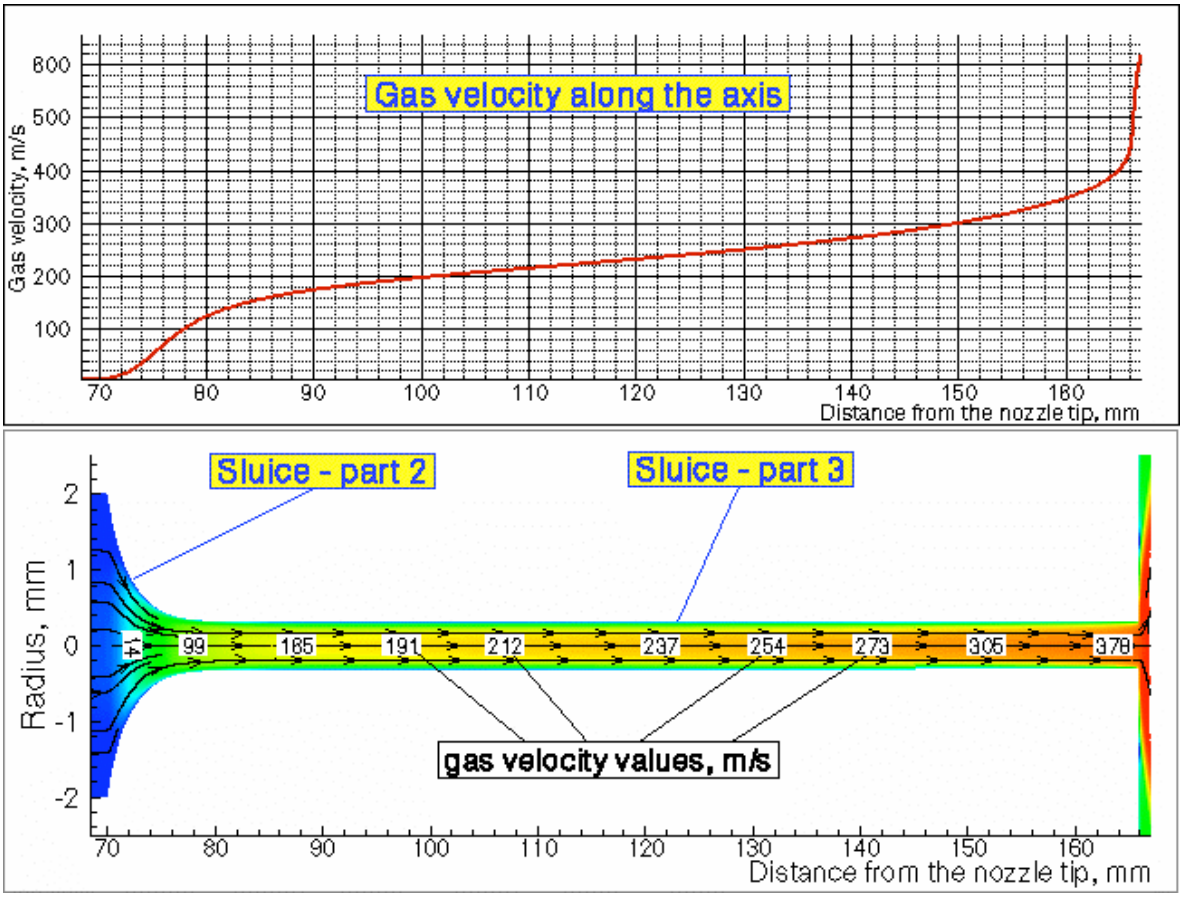

Fig.2. Colored plot of the H_2 buffer gas velocity flow field in the seco0nd and third part of the sluice (bottom): black arrowhead lines are the H_2 gas streamlines; the red color represents maximum and the blue color – minimum velocity values. The gas velocity distribution along the axis is shown in the top.

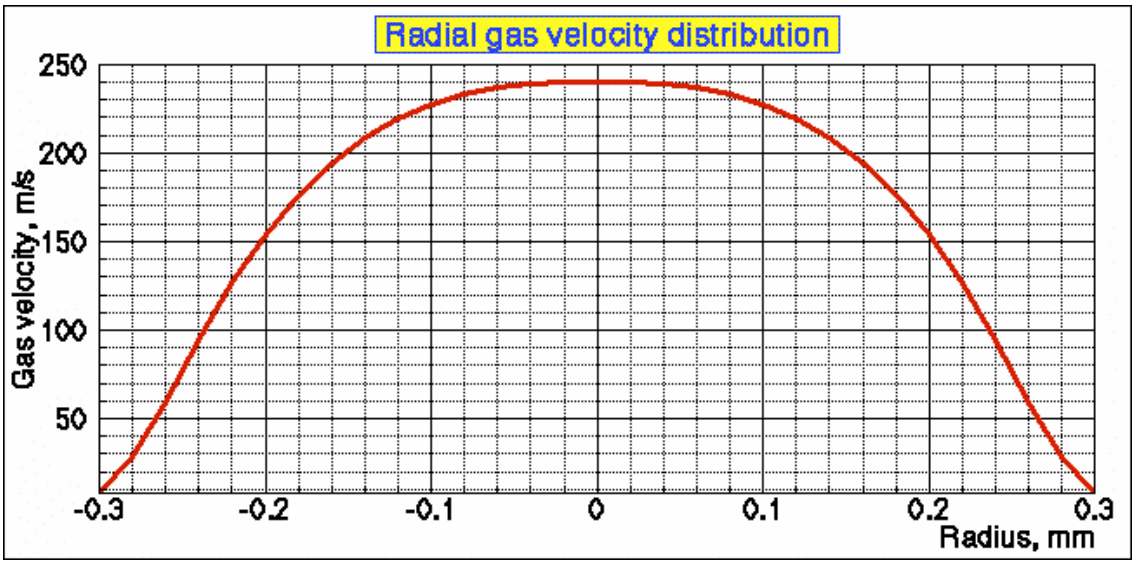

Fig.3. The radial H_2 buffer gas velocity distribution in the middle of the 3rd part of the sluice (see Fig. 2).

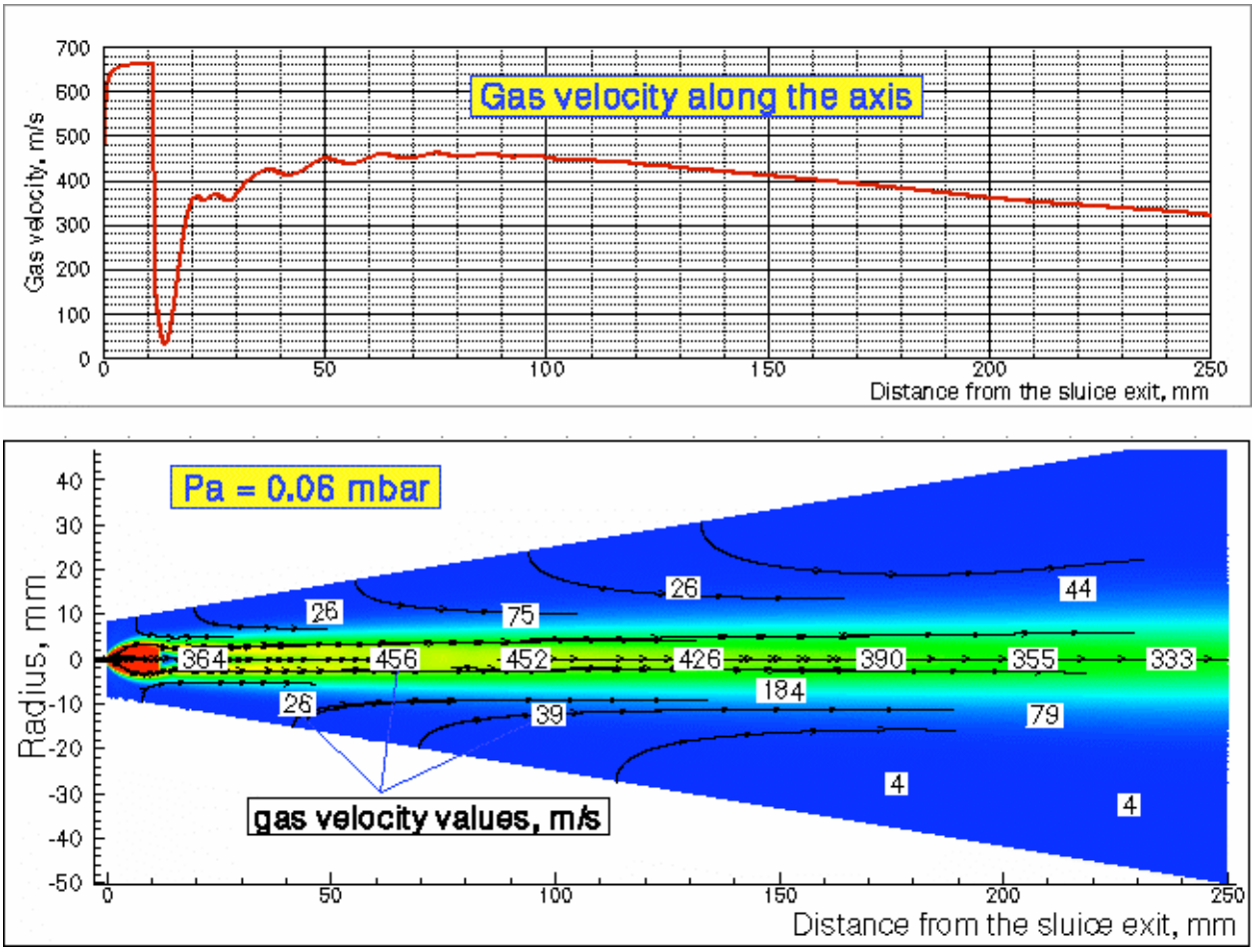

Fig.4. Colored plot of the H_2 buffer gas velocity flow field downstream the sluice exit (bottom): black arrowhead lines are the H_2 gas streamlines; the red color represents maximum and the blue color – minimum velocity values. The ambient pressure P_a = 0.06 mbar. The gas velocity distribution along the axis is shown in the top.

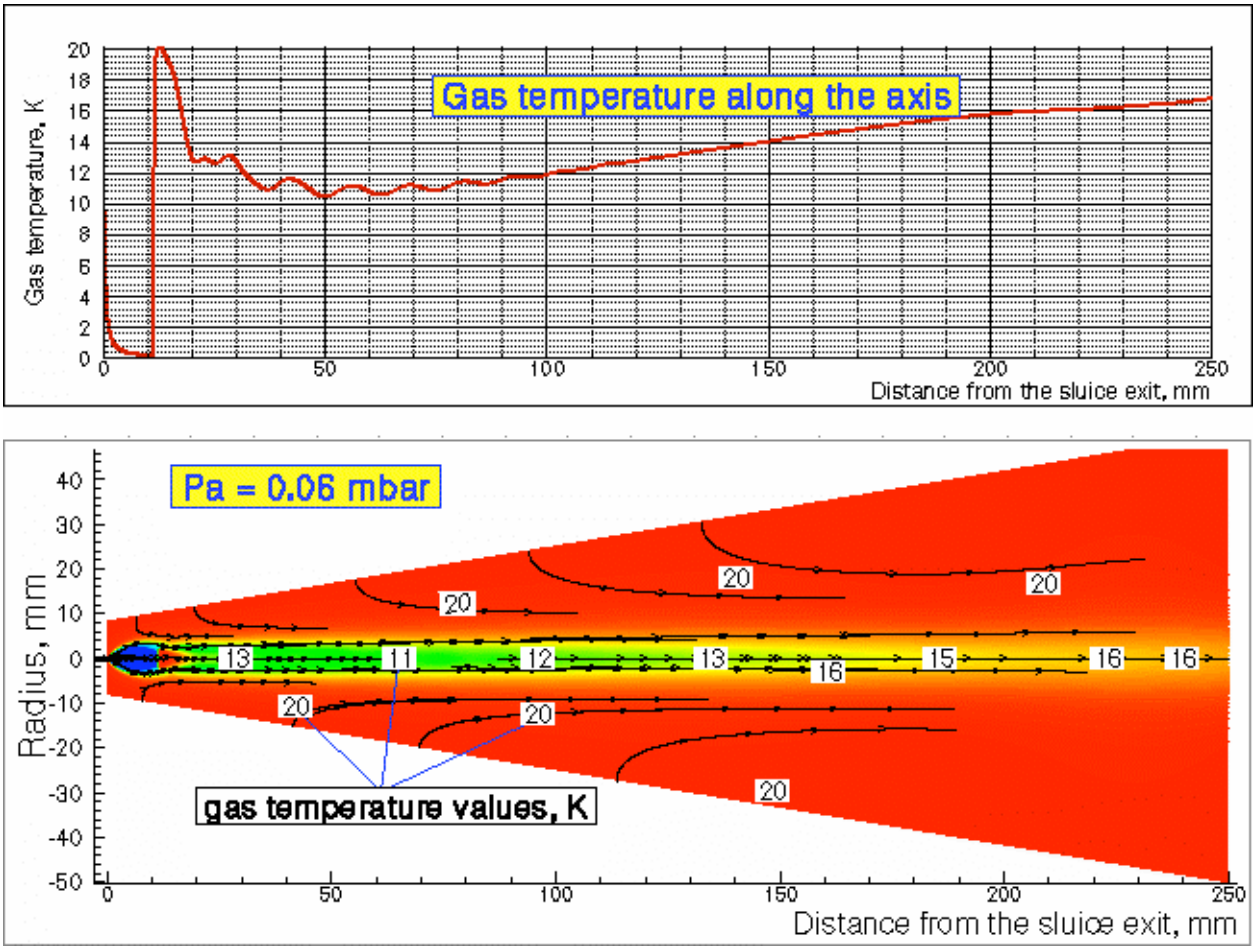

Fig.5. Colored plot of the H_2 buffer gas temperature flow field downstream the sluice exit (bottom): black arrowhead lines are the H_2 gas streamlines; the red color represents maximum and the blue color – minimum temperature values. The ambient pressure P_a = 0.06 mbar. The gas temperature distribution along the axis is shown in the top.

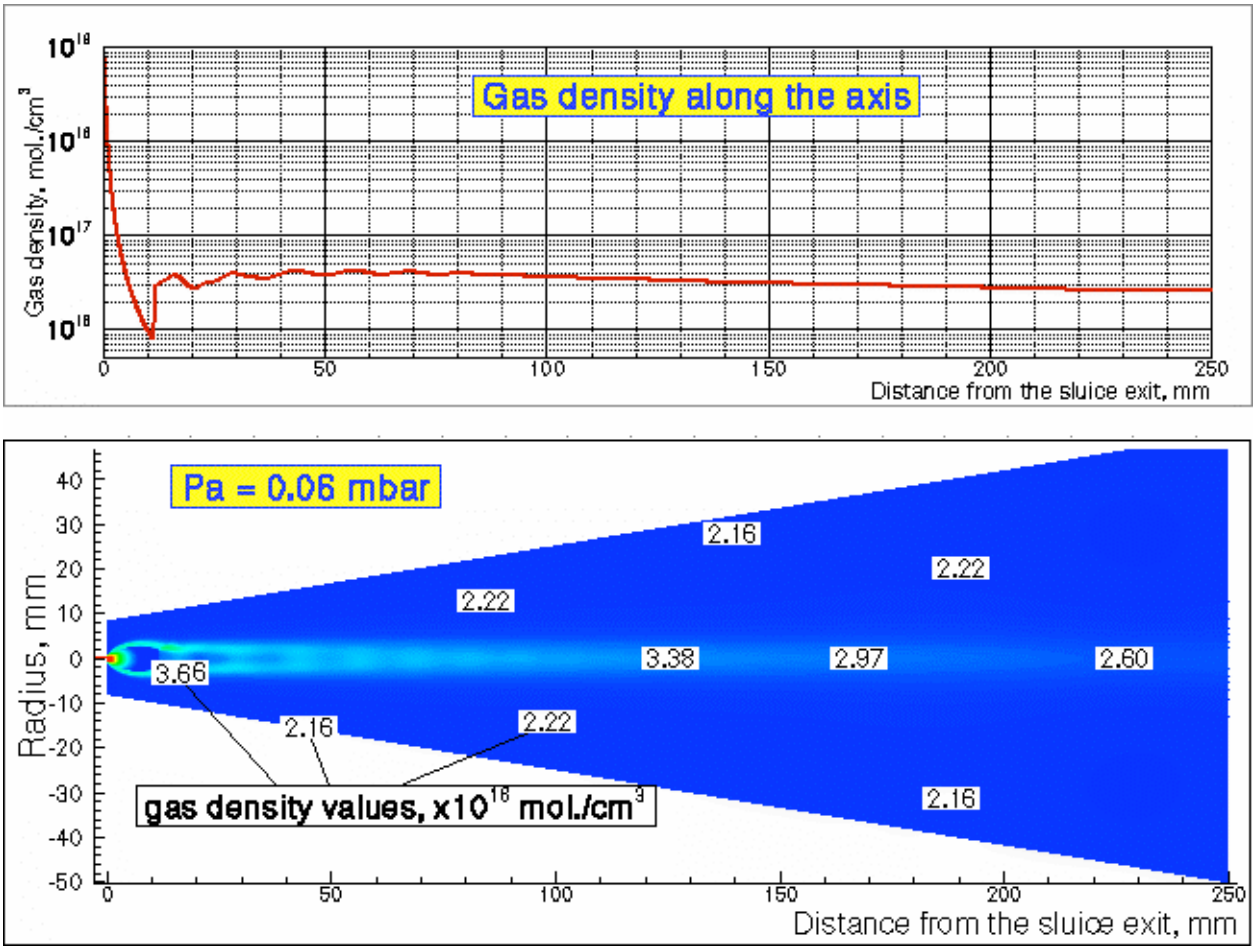

Fig.6. Colored plot of the H_2 buffer gas density flow field downstream the sluice exit (bottom): the red color represents maximum and the blue color – minimum density values. The ambient pressure P_a = 0.06 mbar. The gas density distribution along the axis is shown in the top.

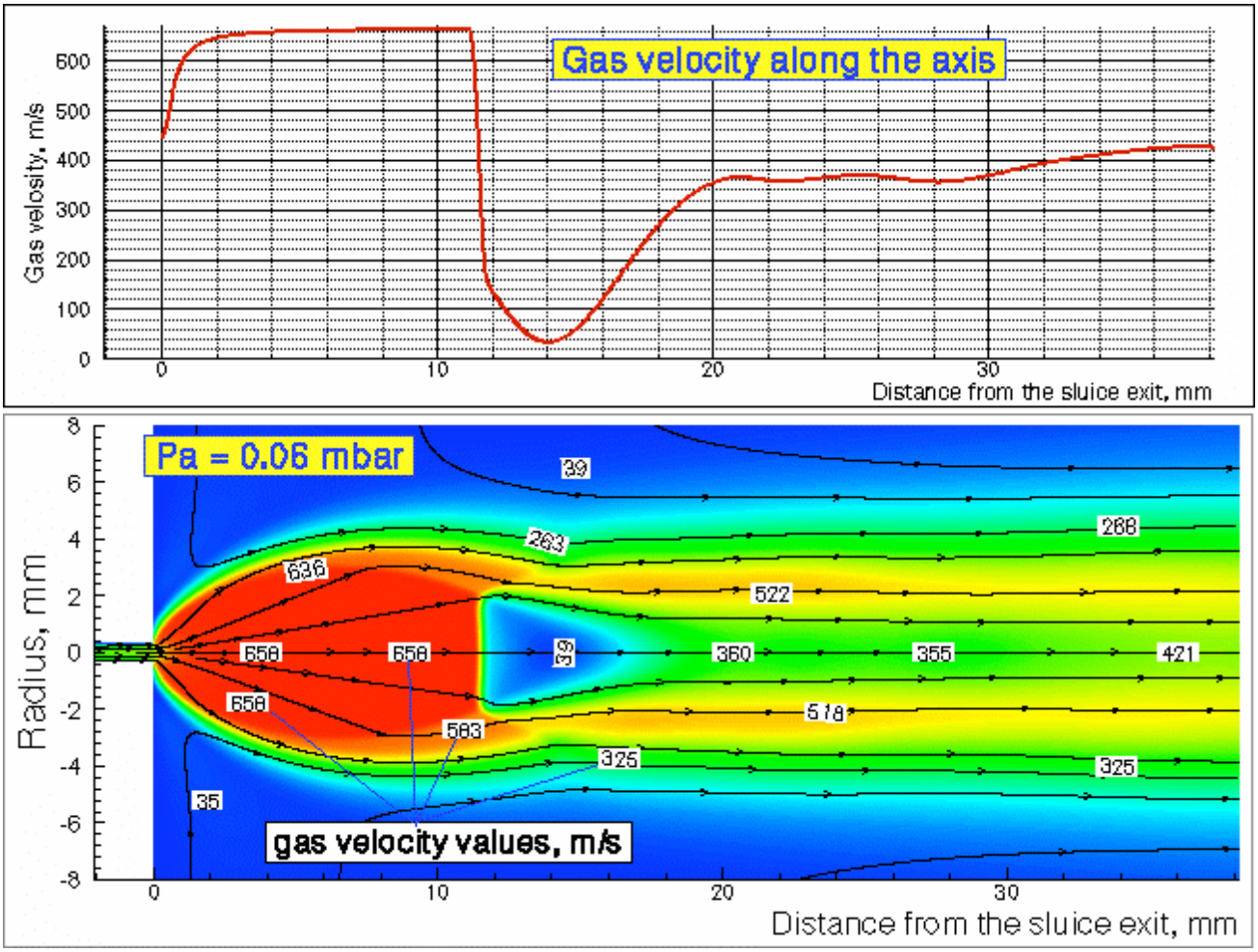

Fig.7. Colored plot of the H_2 buffer gas velocity flow field in vicinity of the sluice exit (bottom): black arrowhead lines are the H_2 gas streamlines; the red color represents maximum and the blue color – minimum velocity values. The ambient pressure P_a = 0.06 mbar. The gas velocity distribution along the axis is shown in the top.

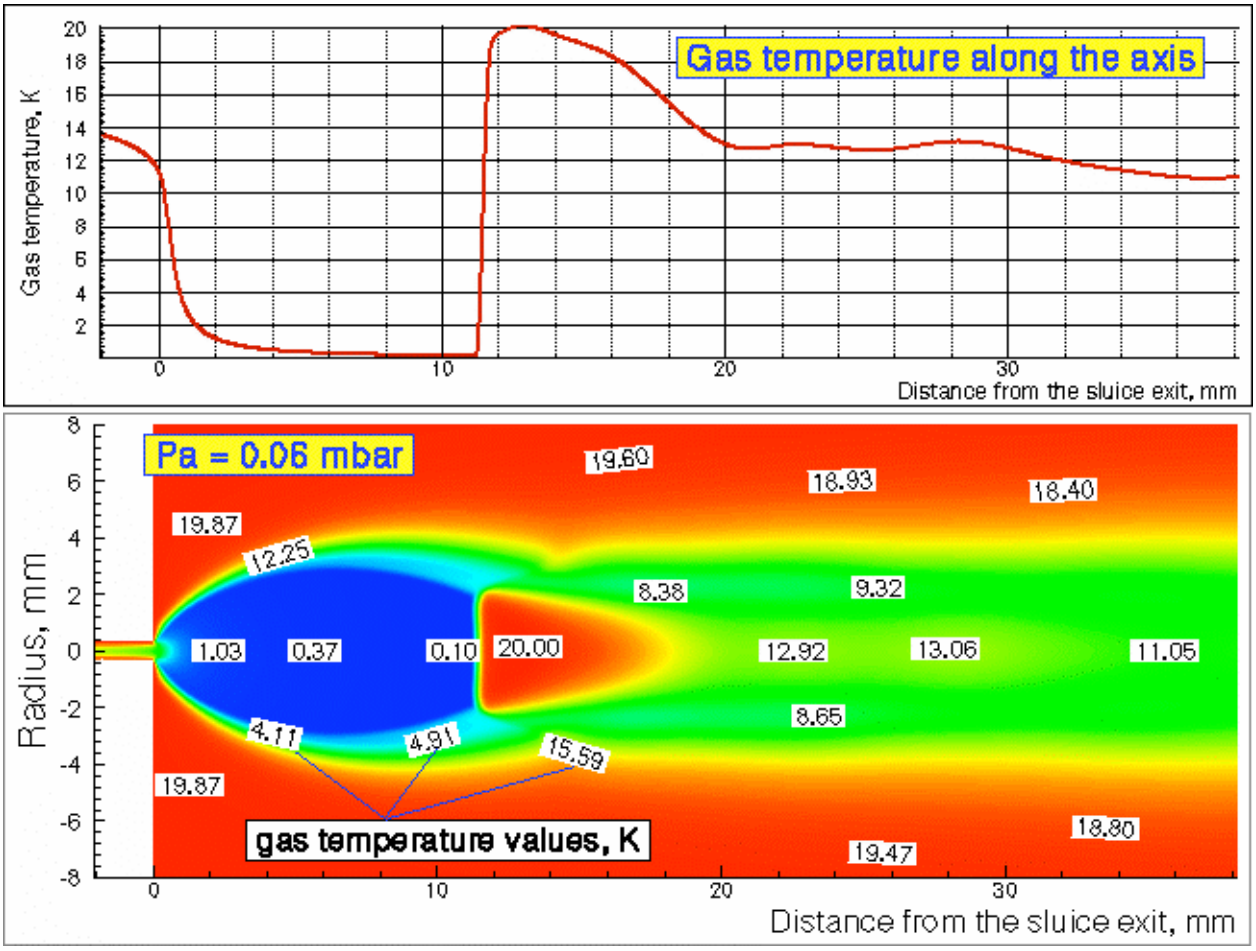

Fig.8. Colored plot of the H_2 buffer gas temperature flow field in vicinity of the sluice exit (bottom): the red color represents maximum and the blue color – minimum velocity values. The ambient pressure P_a = 0.06 mbar. The gas temperature distribution along the axis is shown in the top.

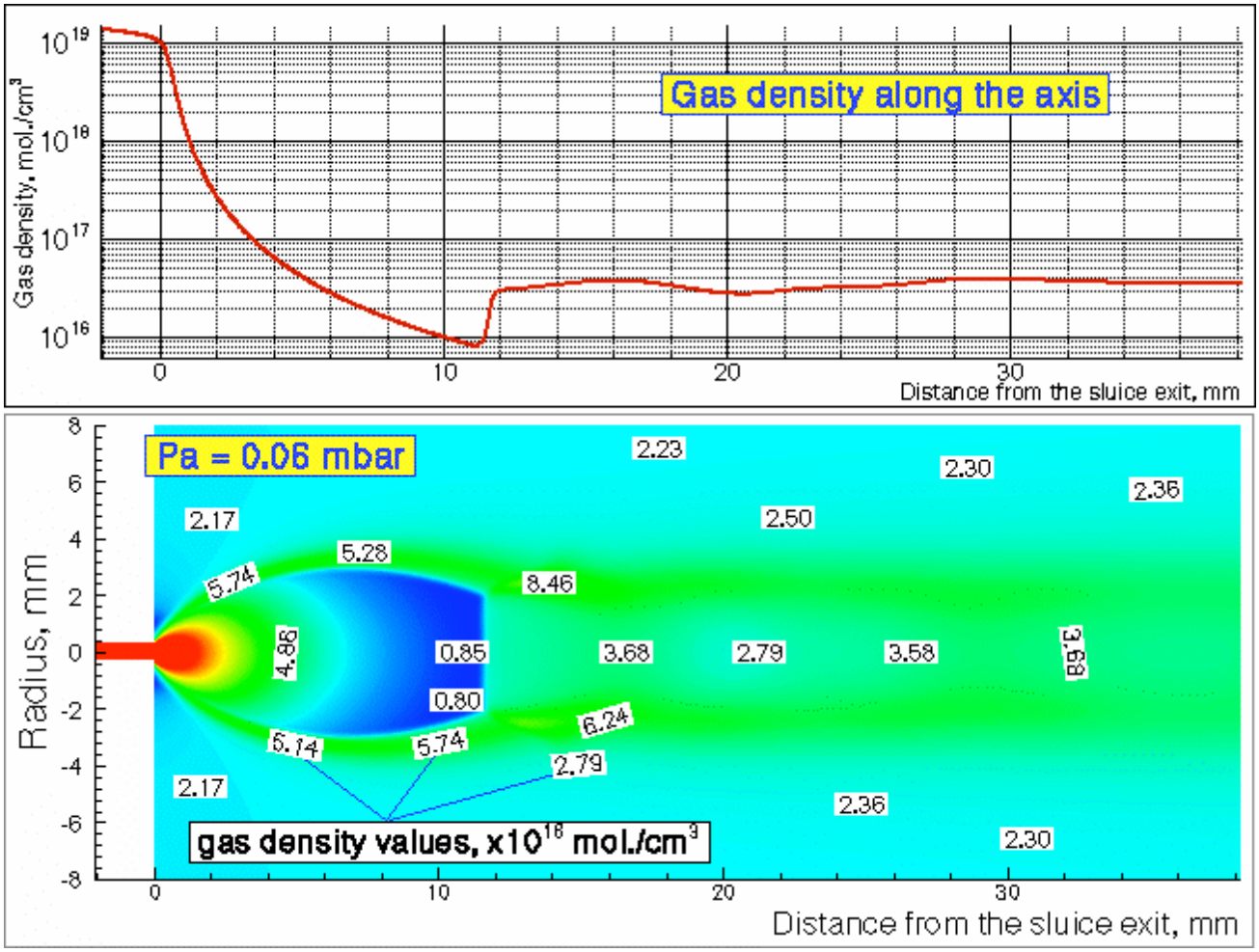

Fig.9. Colored plot of the H_2 buffer gas density flow field in vicinity of the sluice exit (bottom): the red color represents maximum and the blue color – minimum velocity values. The ambient pressure P_a = 0.06 mbar. The gas density distribution along the axis is shown in the top.

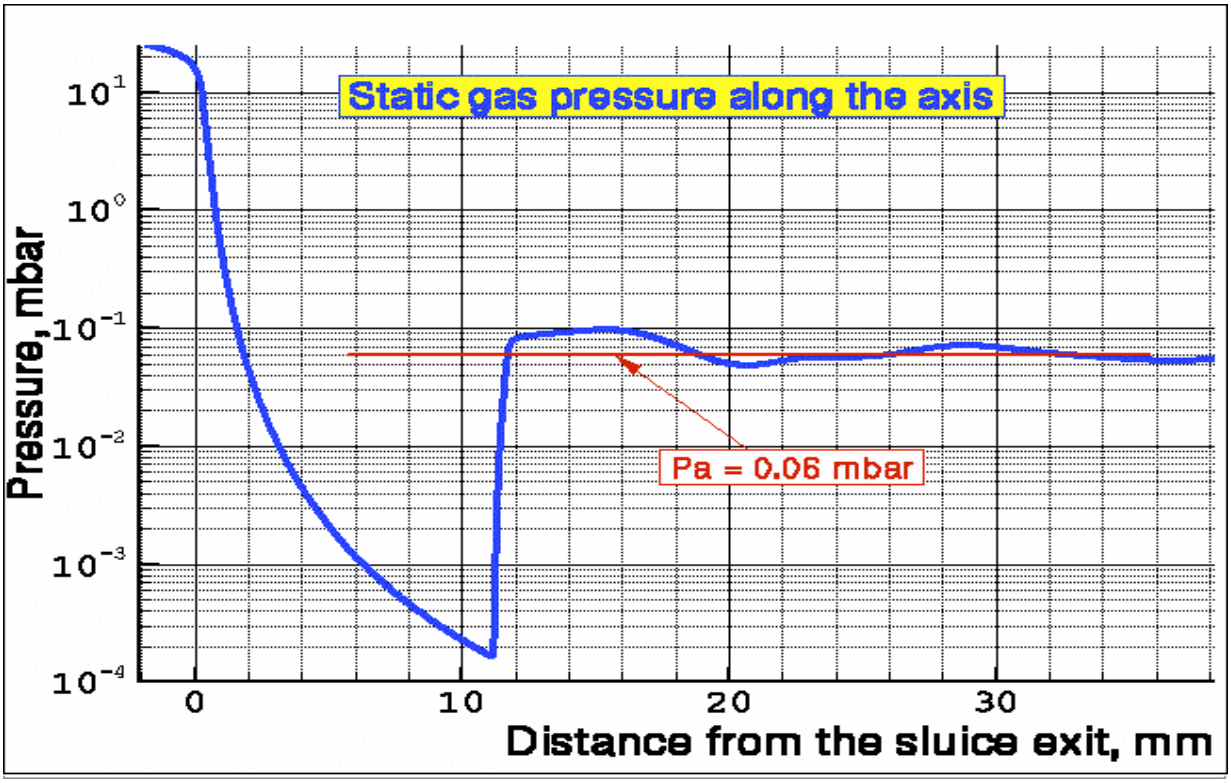

Fig.10. The H_2 buffer gas static pressure distribution along the axis. The ambient pressure P_a = 0.06 mbar that a factor of 300 less than the static gas pressure on the axis of supersonic jet upstream the Mach disk.

3.2 Results of trajectory calculations for the present Moscow-Jülich pellet-generator

Results of trajectory simulations of the droplets (pellets) velocity as a function of the distance from the nozzle are shown in Fig.11. It is suggested here that droplets have a diameter of 20 μm and that after the liquid jet breaks-up into these droplets they start move with an initial velocity V_{in} = 4 m/s along the axis (i.e. an angle between direction of the droplets movement and the axis θ_{in} = 0). The simulation results of the buffer gas velocity distribution along the axis are shown in the Fig. 11 for comparison.

As one can see from the Fig.11, the droplets velocity is considerably increased inside the sluice (in Fig.11 it is the region of 70÷166 mm distances from the nozzle) under the buffer gas drag force. But downstream the sluice exit, where the buffer gas expands into vacuum as a free supersonic jet, the droplets velocity is increased only a little: from 216 m/s at the distance from the nozzle X = 166 mm to the final velocity V_{fin} = 220 m/s at X = 416 mm (it corresponds to the position of the 2nd sluice entrance). This behavior of the droplets downstream the 1st sluice exit is explains by the drastic decreasing of the buffer gas drag force due to the decreasing the buffer gas density by a factor of a thousand (see formula (1) and Figs. 6 and 9).

Fig. 12 shows the details of the first part of the Fig. 11 - it is a region from the nozzle exit to the distance of 45 mm downstream. Notice, that first droplets are decelerated down to velocity of 0.35 m/s at 5.5 mm distance upstream the sluice entrance and then they are accelerated by the gas flow up to 4.2 m/s inside the first part of the sluice.

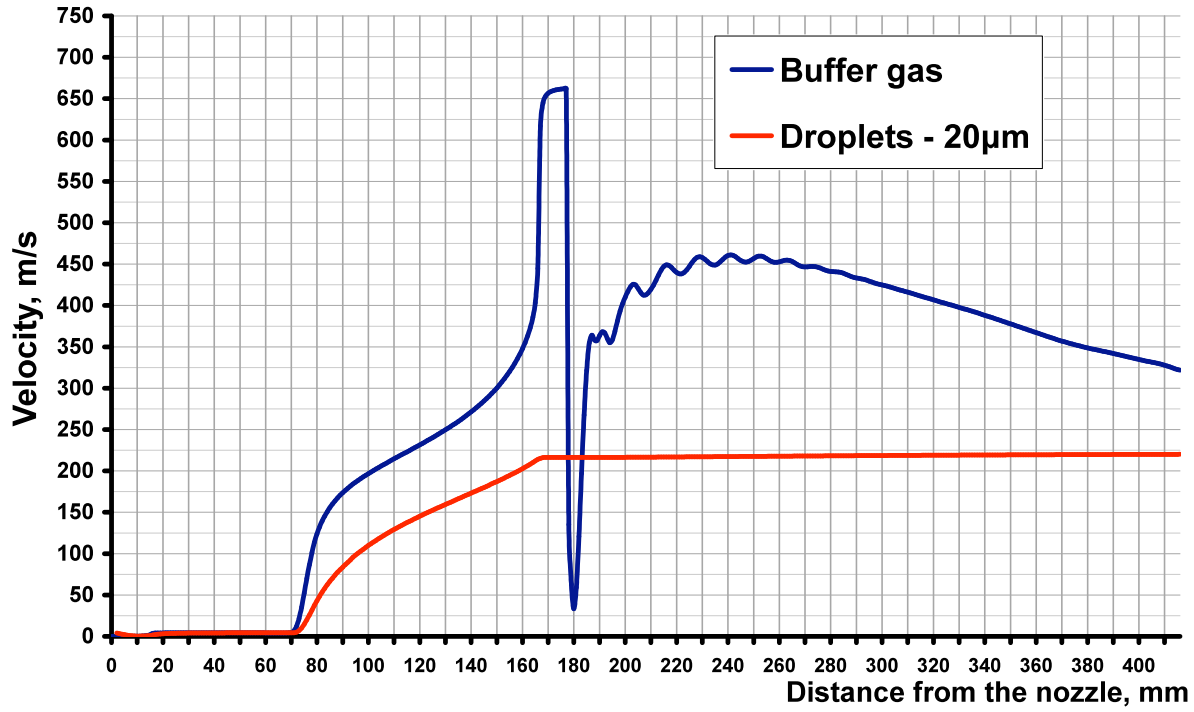

Fig.11. Simulation results of the droplets (pellets) velocity as a function of the distance from the nozzle (red line). Droplets have a diameter 20 μm, an initial velocity V_{in} = 4 m/s and move along the axis. The simulation results for the buffer gas velocity distribution along the axis (blue line) are shown for comparison.

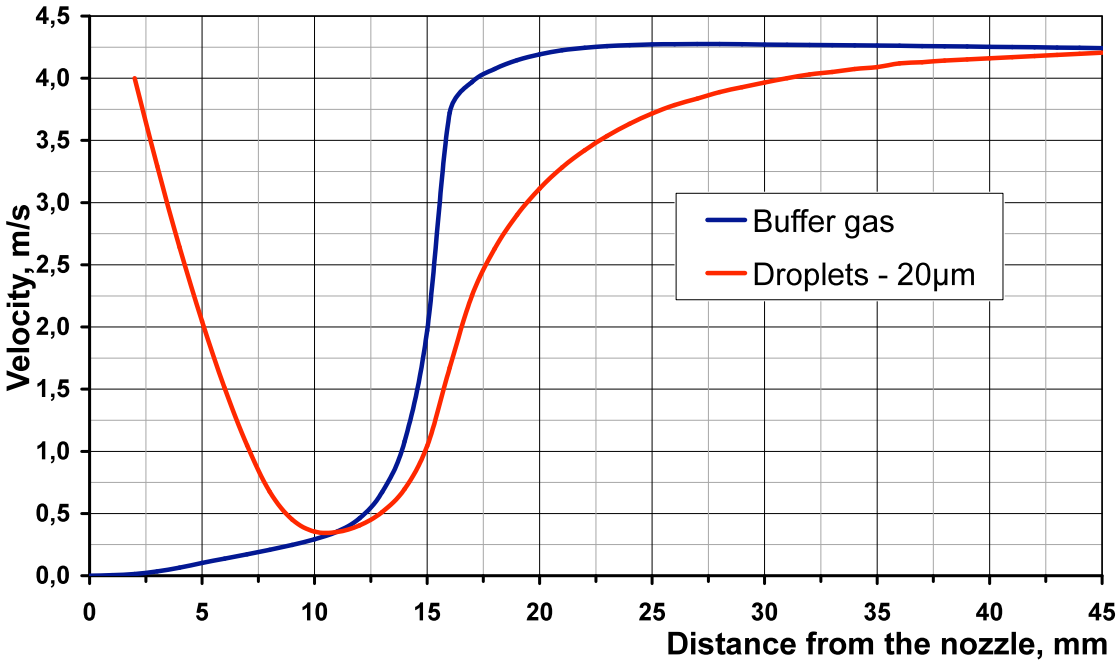

Fig.12. Simulation results of the droplets velocity as a function of the distance from the nozzle (red line). Droplets have a diameter 20 μm, an initial velocity V_{in} = 4 m/s and move along the axis. The simulation results for the buffer gas velocity distribution along the axis (blue line) are shown for comparison.

The results of calculations for a pellet final velocity as a function of pellet diameter are shown in Fig.13.

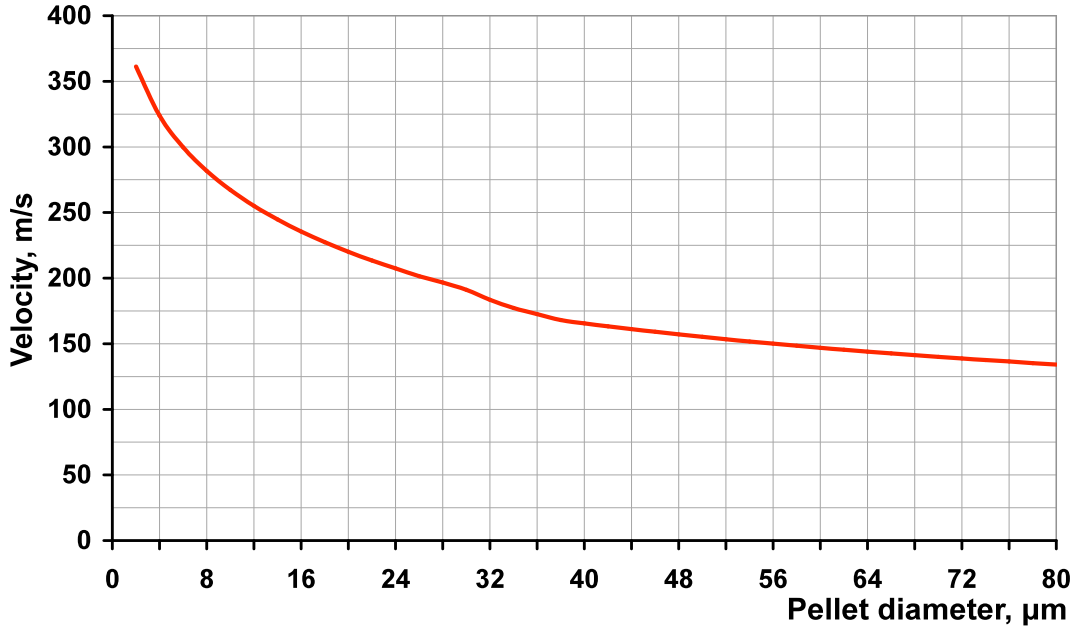

Fig.13. Pellet final velocity as a function of the pellet diameter. The initial droplets velocity V_{in} = 4 m/s.

A decreasing of the pellet velocity with the pellet diameter is simply explains by an inertia effect.

Because I did not have data about initial droplet-beam angular divergence after the liquid jet decay, I have decided perform computer trajectory simulations for droplets, which start to move in the buffer gas at various angles θ_{in} to the axis. Fig.14 shows results of simulations of three trajectories of the droplets, which start to move at the following initial angles to the axis: θ_{in} = 50 mrad, θ_{in} = 100 mrad and θ_{in} = 150 mrad. The droplets diameter and the initial velocity are equal to 20 μm and 4 m/s, correspondingly.

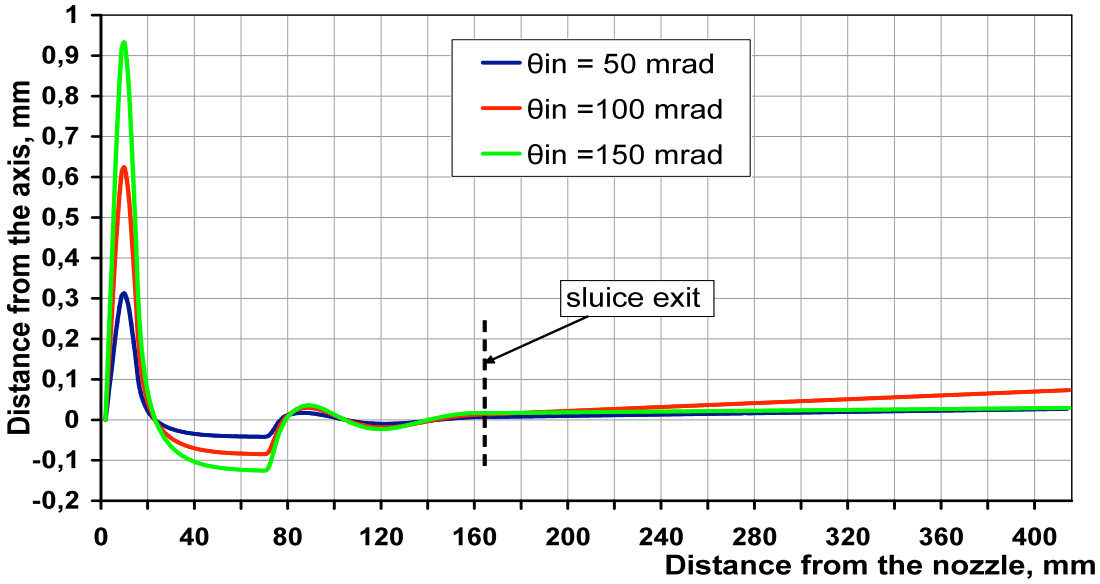

Fig.14. Simulation results of trajectories of the droplets, which start to move at different initial angles θ_{in} to the axis. The droplets have a diameter of 20 μm, its initial velocity V_{in} = 4 m/s.

A strong focusing effect of the buffer gas flow is clear visible. A more detailed view of these trajectories inside the sluice is shown in Fig.15.

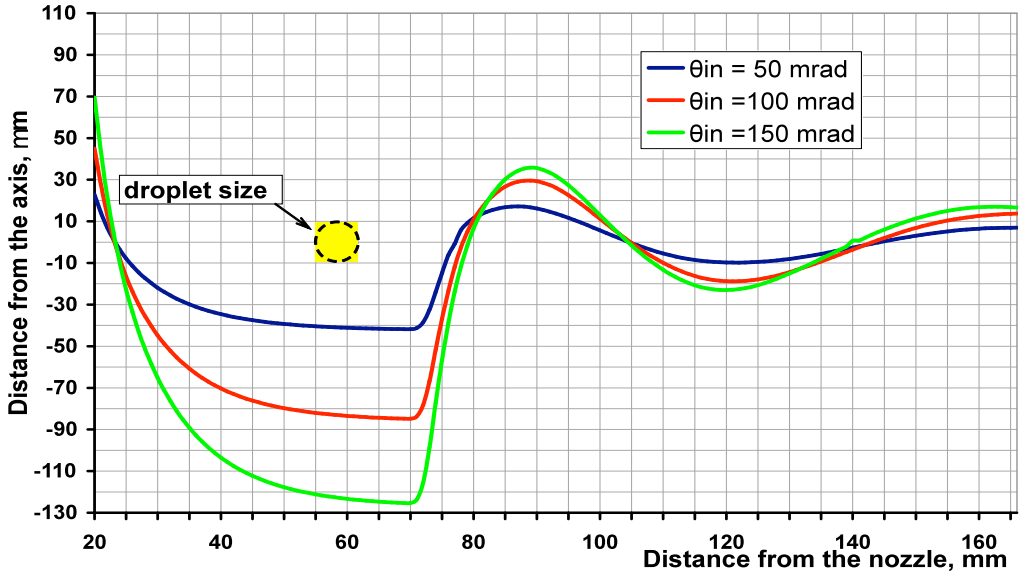

Fig.15. A more detailed view of the droplet trajectories inside the sluice. A droplet size is shown as a yellow circle for illustration.

4. HOW EASILY IMPROVE THE PELLET-GENERATOR PERFORMANCE

After an analysis of the obtained results I have made a conclusion that a performance of the Moscow-Jülich pellet-generator can be easily improved. For this purpose it will be enough just to make some changes into the 1st sluice design.

First, it looks reasonable to decrease the distance between the nozzle exit and the sluice entrance (now it is 16 mm) because the droplets are decelerated down to the buffer gas velocity already at 5.5 mm distance upstream the sluice entrance (see Figs. 12).

Second, taking into account that there is no droplets focusing inside the long first part of the sluice (this part of the sluice has 54 mm length and 4 mm inner diameter) – thermalized in the buffer gas droplets move here parallel to the tube axis with about constant velocities, which values depend on a distance from the tube axis (see Fig. 1) – one can considerably shorten this tube and, in addition, decrease its inner diameter.

Third (and most important), I recommend decrease the inner diameter of the exit part of the sluice (now it is a glass tube of 81 mm length and of 0.6 mm inner diameter). It will not lead to the droplet-beam losses inside the sluice (see Fig. 15), just quite the contrary the smaller inner diameter of this tube will allow reduce the buffer gas load into the vacuum chamber behind the sluice exit.

Of course, the entrance and exit diameter of the exponential (the second or transitional) part of the sluice should be adjusted to the new diameter values of the first and exit sluice part.

Forth, instead of the 2nd sluice that installed at big distance from the exit of the 1st sluice (now this distance is 250 mm) I recommend to use a skimmer with a small entrance aperture (e.g. it may be a commercially available skimmer from Beam Dynamic – see for details Ref. [17]) placed on the supersonic buffer gas-jet axis upstream the Mach disk (see Figs. 7-10).

To check how these changes can help to improve the performance of the Moscow-Jülich pellet-generator I have performed the gas dynamic and trajectory simulations for the following new sluice geometry:

- distance between the nozzle exit and the sluice entrance is 9 mm;

- the first part of the sluice is a cylindrical tube of 5 mm length with inner diameter of 2 mm;

- the second (transitional) sluice part of 13.5 mm length has an inner diameter that decreases exponentially from 2 mm to 0.4 mm in the buffer gas flow direction;

- the third (exit) part of the sluice of 81 mm length has an inner diameter of 0.4 mm.

The buffer gas operation conditions in these simulations are the same as they are for the present Moscow-Jülich pellet-generator: the stagnation hydrogen buffer gas temperature and pressure are equal to 20 K and 100 mbar, correspondingly; the ambient pressure in the vacuum chamber behind the new sluice exit is 0.06 mbar; velocity of the liquid jet V_{jet} = 4 m/s, which length is in the range of 1÷5 mm.

The results of calculations for new sluice geometry are presented in the two next sections.

4.1 Results of gas dynamic calculations for new sluice geometry

Figs. 16-17 show results of calculation for the H_2 buffer gas velocity flow field in different parts of the new sluice.

The results of gas dynamic simulations for gas flow fields of velocity, temperature and density in the vacuum chamber downstream the new sluice exit are shown in Figs. 18, 19 and 20, correspondingly. Fig. 21 shows the H_2 buffer gas static pressure distribution along the axis in this vacuum chamber.

As one can see in the Figs. 18-21, the structure of the supersonic gas-jet here differ from that one of the present Moscow-Jülich sluice (see Figs.7-10). E.g. the position of the Mach disk here corresponds to ~5.5 mm distance from the sluice exit that is twice less than it is in the case of the present Moscow-Jülich pellet-generator.

The buffer gas flow rate through the new sluice $Q_{sluice} = 2.39 \cdot 10^{20}$ mol./s that corresponds to 9.9 mbar l/s at room temperature. So, to maintain $6 \cdot 10^{-2}$ mbar ambient pressure in the vacuum chamber behind the new sluice it will be enough to use a Roots pump of 165 l/s pumping speed.

It is common knowledge that for the best skimming the skimmer should be placed inside the supersonic gas-jet upstream the Mach disk position. So, in the case of the Moscow-Jülich pellet-generator operation with the new sluice it will be reasonable to install the skimmer at ~5 mm distance from the sluice exit. As to an optimum skimmer aperture diameter, it should satisfy a condition, when a Knudsen number $Kn \geq 1$ (the Knudsen number here is determined as a ratio of the mean free pass length of the hydrogen gas molecules λ_{gas} to the skimmer diameter). In our case it corresponds to the skimmer with 0.2 mm aperture. In this case the gas load into the next high-vacuum chamber (behind the skimmer) will be about $Q_{skim} = 1.7 \cdot 10^{17}$ mol./s that corresponds to $7 \cdot 10^{-3}$ mbar l/s at room temperature. As a result, the pellets can be extracted into high-vacuum conditions (~$3 \cdot 10^{-5}$ mbar) with the use of a small turbo molecular pump of ~200÷300 l/s. Notice, that the background pressure behind the 2nd skimmer in the present Moscow-Jülich pellet-target setup is $1 \cdot 10^{-3}$ mbar (unfortunately, I do not know what vacuum pumps are used to maintain this pressure).

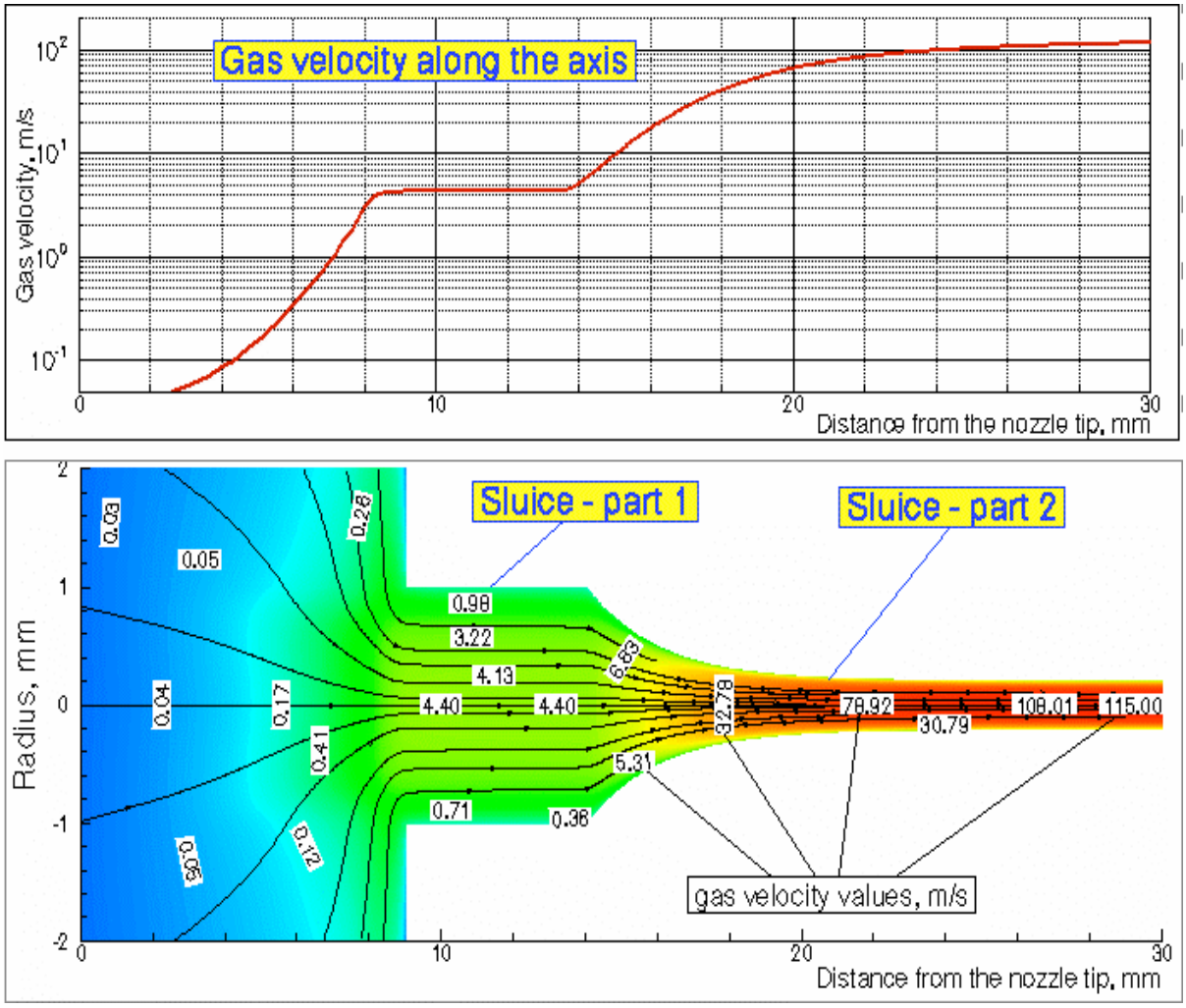

Fig.16. Colored plot of the H_2 buffer gas velocity flow field in the region from the nozzle exit to the new sluice entrance and inside the first and second parts of this sluice (bottom): black arrowhead lines are the H_2 gas streamlines; the red color represents maximum and the blue color – minimum velocity values. The gas velocity distribution along the axis is shown in the top.

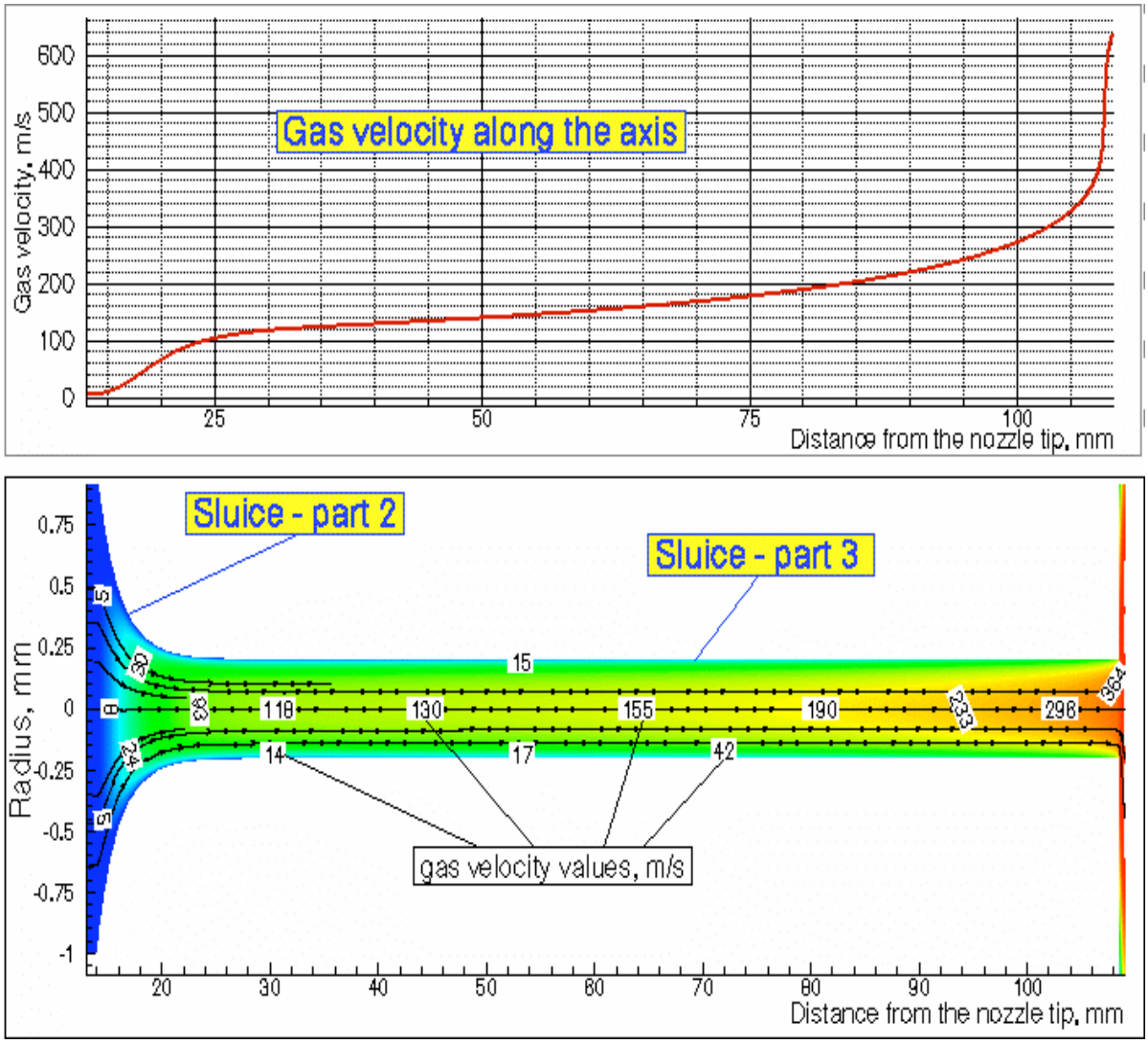

Fig.17. Colored plot of the H_2 buffer gas velocity flow field in the second and third part of new sluice (bottom): black arrowhead lines are the H_2 gas streamlines; the red color represents maximum and the blue color – minimum velocity values. The gas velocity distribution along the axis is shown in the top.

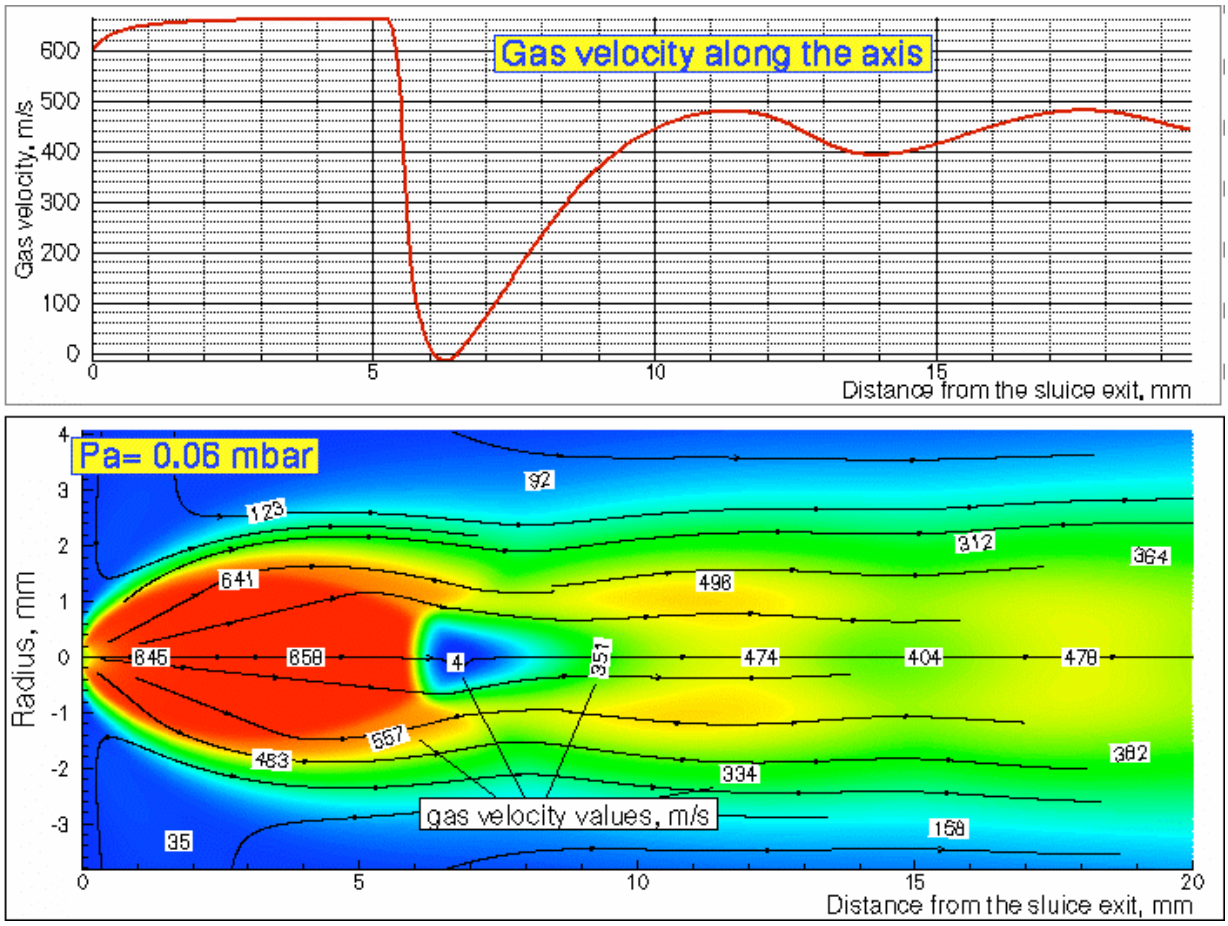

Fig.18. Colored plot of the H_2 buffer gas velocity flow field behind the new sluice exit (bottom): black arrowhead lines are the H_2 gas streamlines; the red color represents maximum and the blue color – minimum velocity values. The ambient pressure P_a = 0.06 mbar. The gas velocity distribution along the axis is shown in the top.

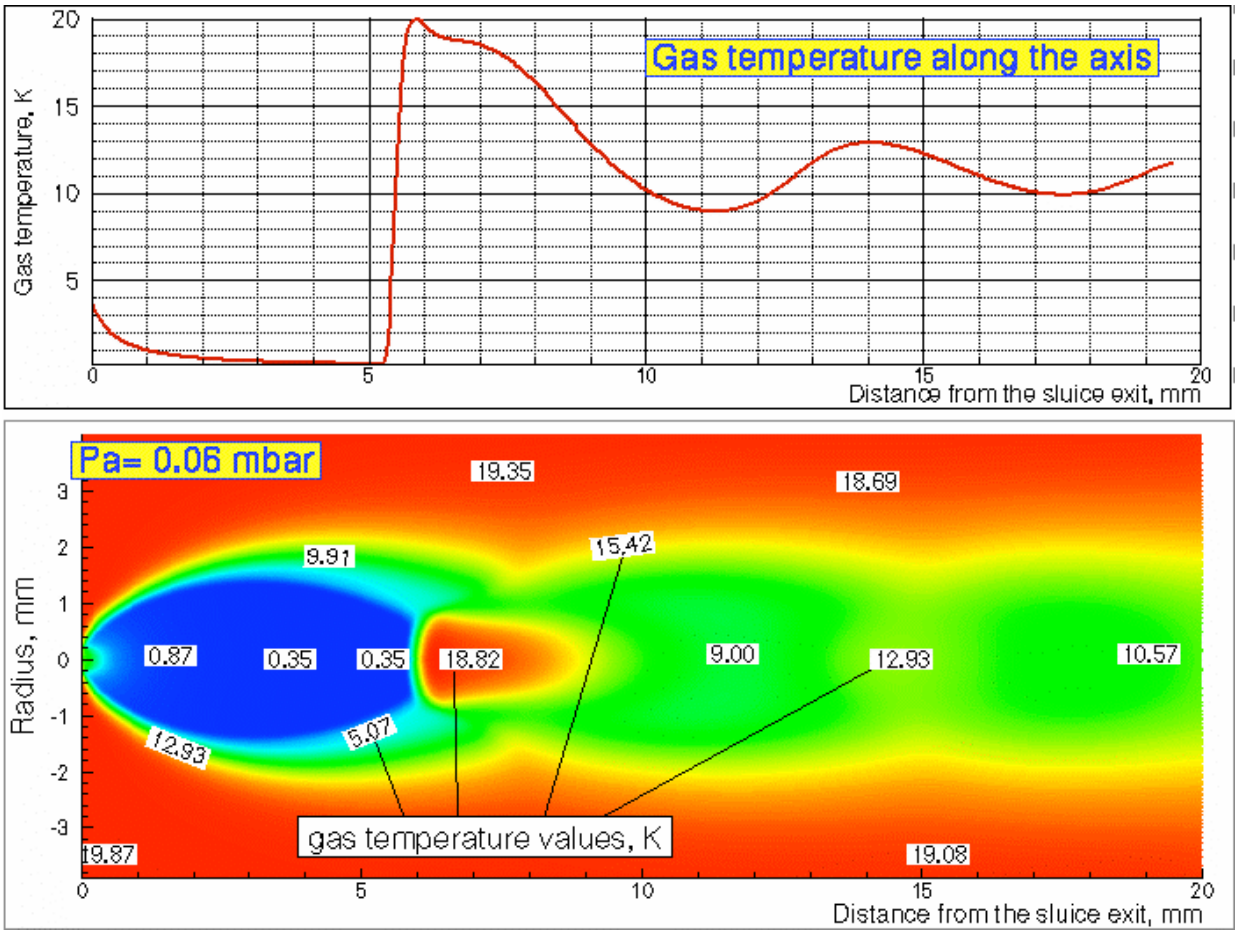

Fig.19. Colored plot of the H_2 buffer gas temperature flow field behind the new sluice exit (bottom): the red color represents maximum and the blue color – minimum velocity values. The ambient pressure P_a = 0.06 mbar. The gas temperature distribution along the axis is shown in the top.

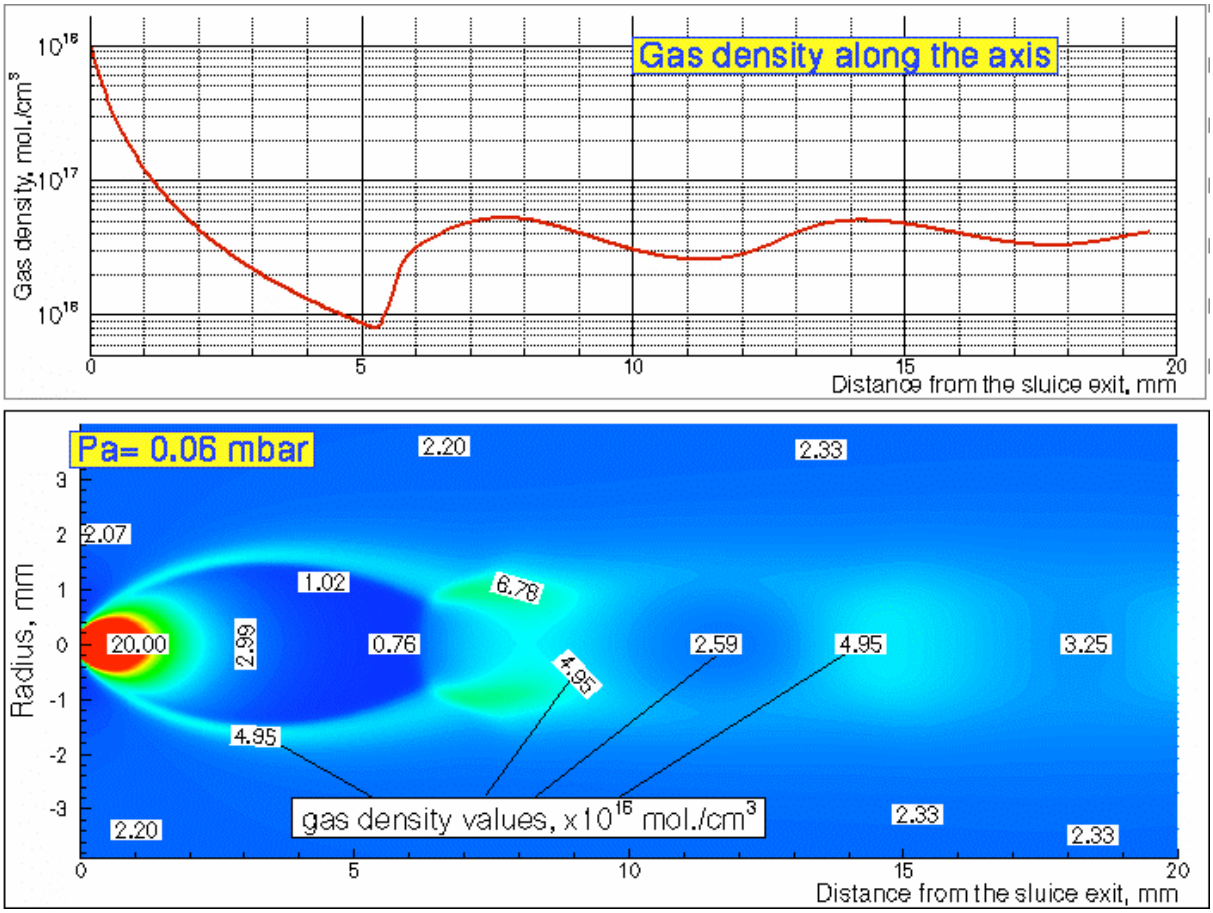

Fig.20. Colored plot of the H_2 buffer gas density flow field behind the new sluice exit (bottom): the red color represents maximum and the blue color – minimum velocity values. The ambient pressure P_a = 0.06 mbar. The gas density distribution along the axis is shown in the top.

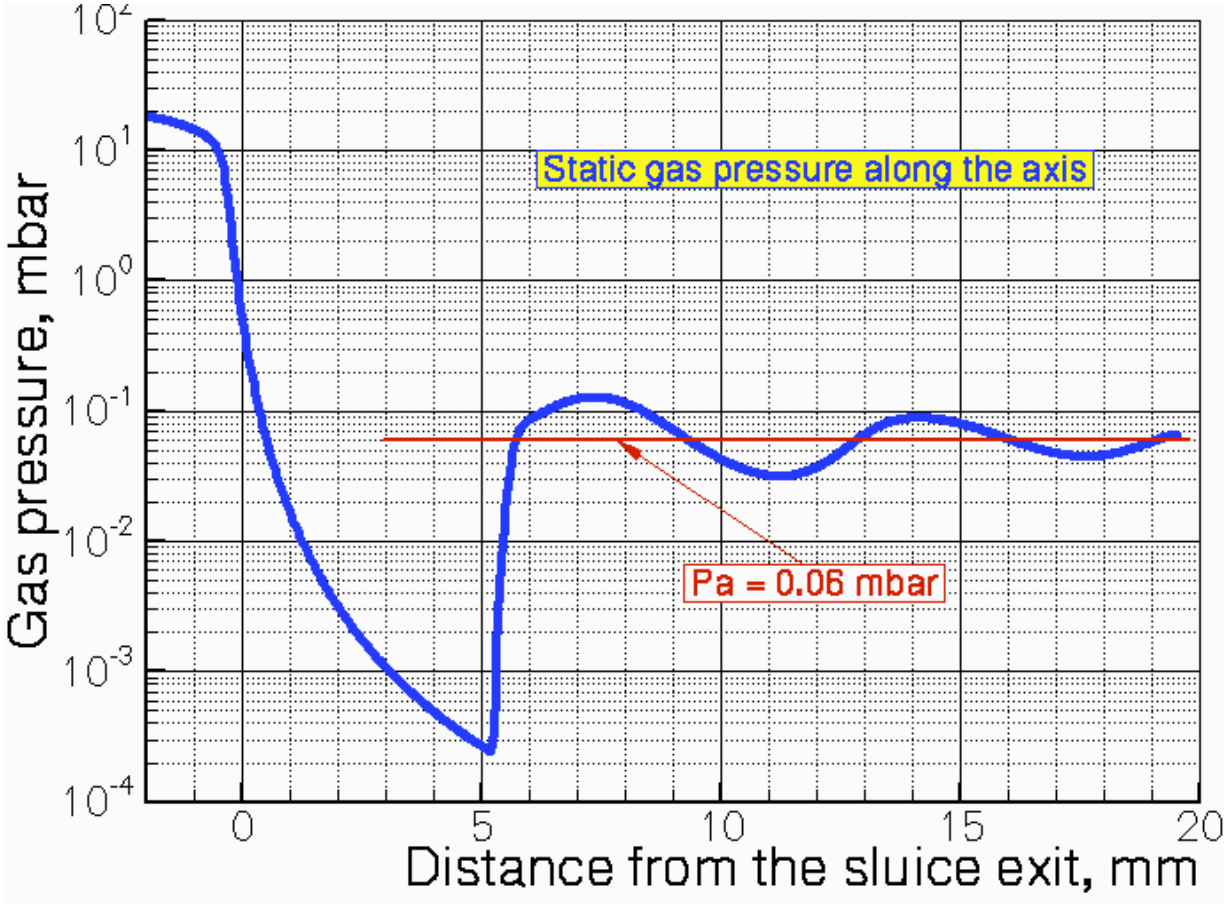

Fig.21. The H_2 buffer gas static pressure distribution along the new sluice axis. The ambient pressure P_a = 0.06 mbar, that about a factor of 200 less than the static gas pressure on the axis of supersonic jet in front of the Mach disk.

4.2 Results of trajectory calculations for new sluice geometry

Results of trajectory simulations for the droplets (pellets) velocity as a function of the distance from the nozzle are shown in Fig.22. It is suggested here that droplets have a diameter 20 μm and that after the liquid jet breaks-up into these droplets they start to move with an initial velocity V_{in} = 4 m/s along the axis. The final pellets velocity at 5 mm distance from the new sluice exit (where the skimmer should be placed) V_{fin} = 165 m/s. The simulation results for the buffer gas velocity distribution along the axis are shown in the Fig. 22 for comparison.

Fig.23 shows the details of the Fig. 11 for a region between the nozzle exit and 16 mm distance downstream. Notice, that droplets here decelerate in the buffer gas down to 1 m/s velocity at about 1 mm distance from the new sluice entrance (in accordance with my simulations for the present Moscow-Jülich sluice geometry droplets decelerate down to 0.35 m/s velocity – see Fig.12).

The results of calculations for a pellet final velocity as a function of pellet diameter are presented in Fig.24.

Similar to the Figs.14 and 15, the results of simulations of three trajectories of the droplets, which start to move at different initial angles θ_{in} to the axis, are presented in Figs. 25 and 26 for the case of new sluice geometry. The droplets diameter and the initial velocity are equal to 20 μm and 4 m/s, correspondingly. As one can see in the Fig.26, amplitudes of trajectories oscillations inside the new sluice are considerably less than that one inside of the present Moscow-Jülich sluice (see Fig. 15 for comparison).

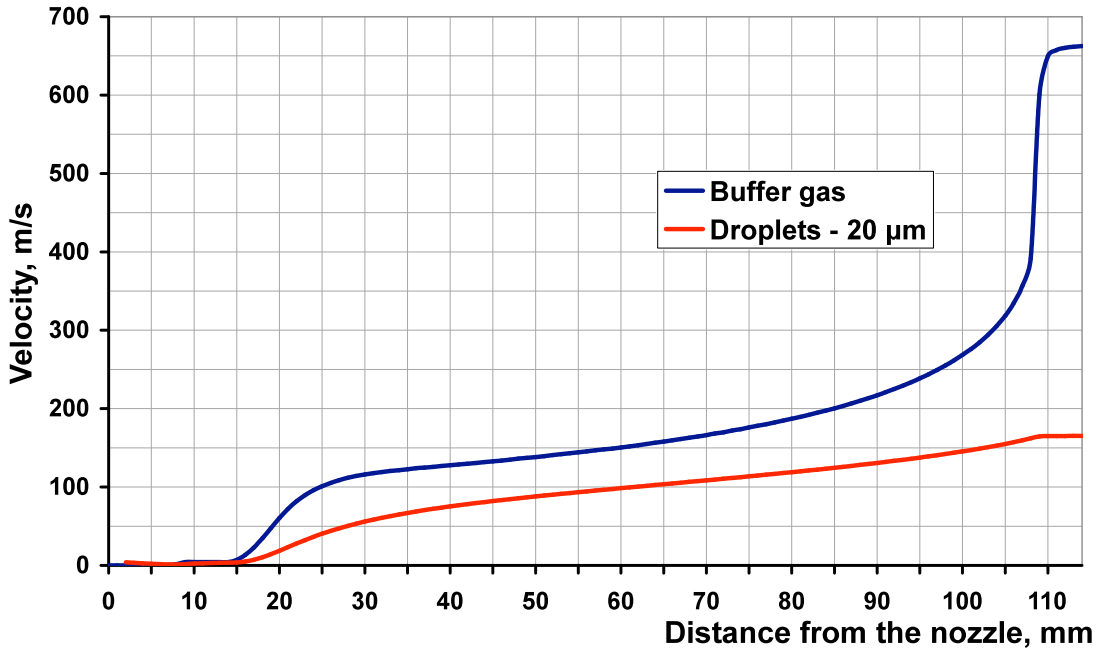

Fig.22. Simulation results of the droplets (pellets) velocity as a function of the distance from the nozzle (red line). Droplets have a diameter 20 μm, the initial velocity V_{in} = 4 m/s and move along the axis. The simulation results for the buffer gas velocity distribution along the axis (blue line) are shown for comparison.

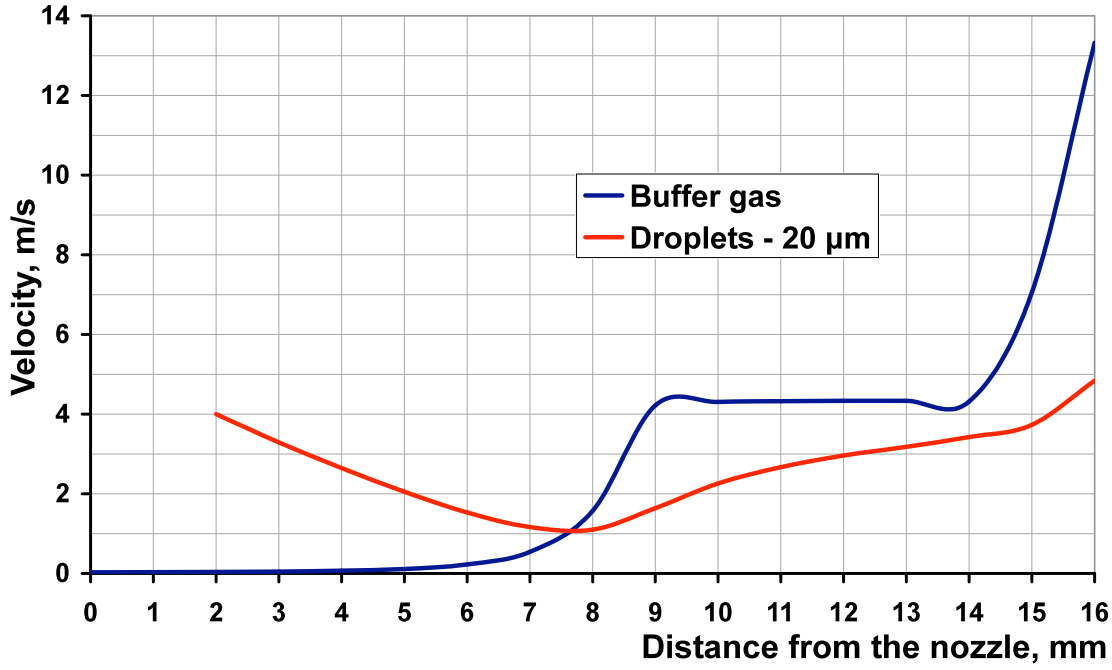

Fig.23. Simulation results of the droplets velocity as a function of the distance from the nozzle (red line). Droplets have a diameter 20 μm, an initial velocity V_{in} = 4 m/s and move along the axis. The simulation results for the buffer gas velocity distribution along the axis (blue line) are shown for comparison.

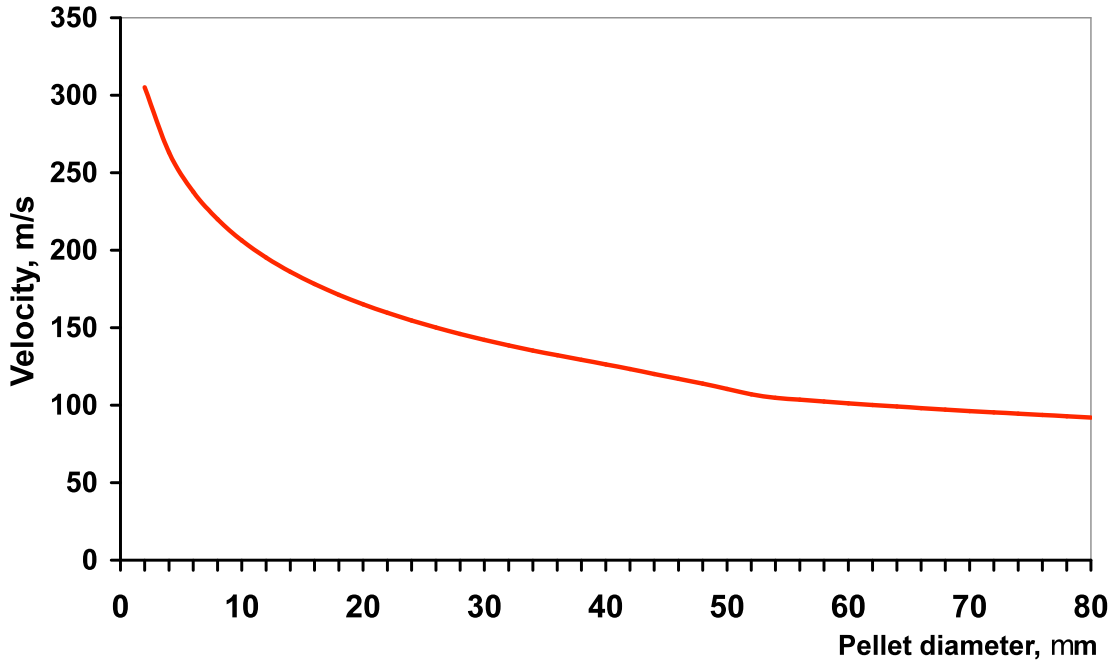

Fig.24. Pellet final velocity as a function of the pellet diameter. The initial droplets velocity V_{in} = 4 m/s.

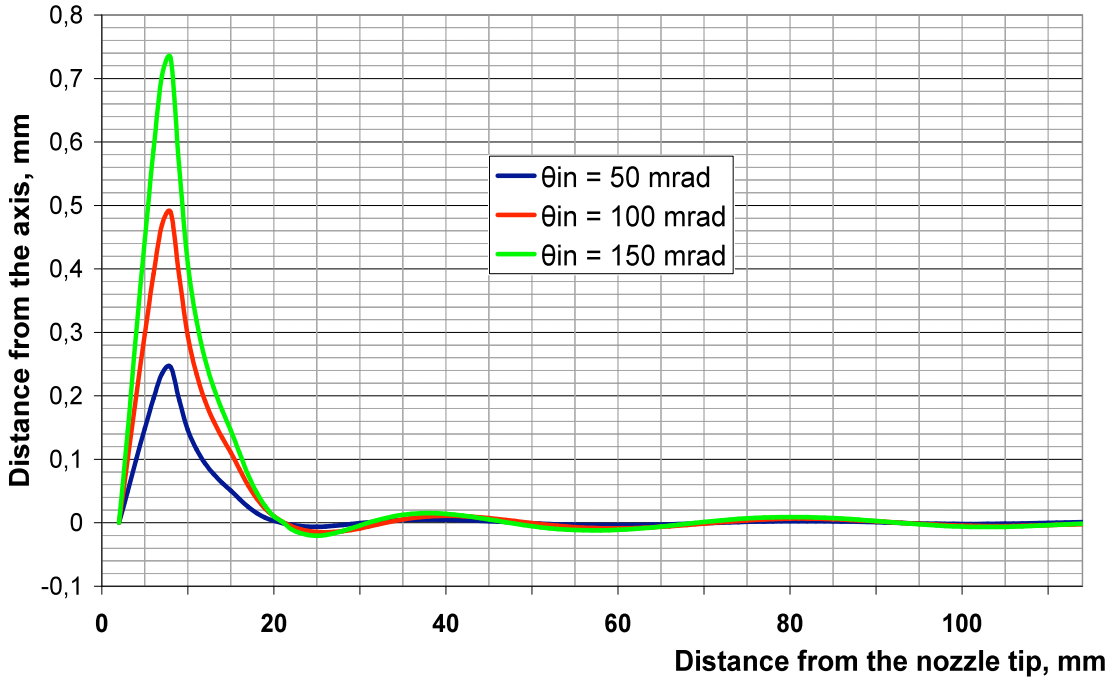

Fig.25. Simulation results of trajectories of the droplets, which start to move at different initial angles θ_{in} to the axis. The droplets have a diameter of 20 μm, its initial velocity V_{in} = 4 m/s.

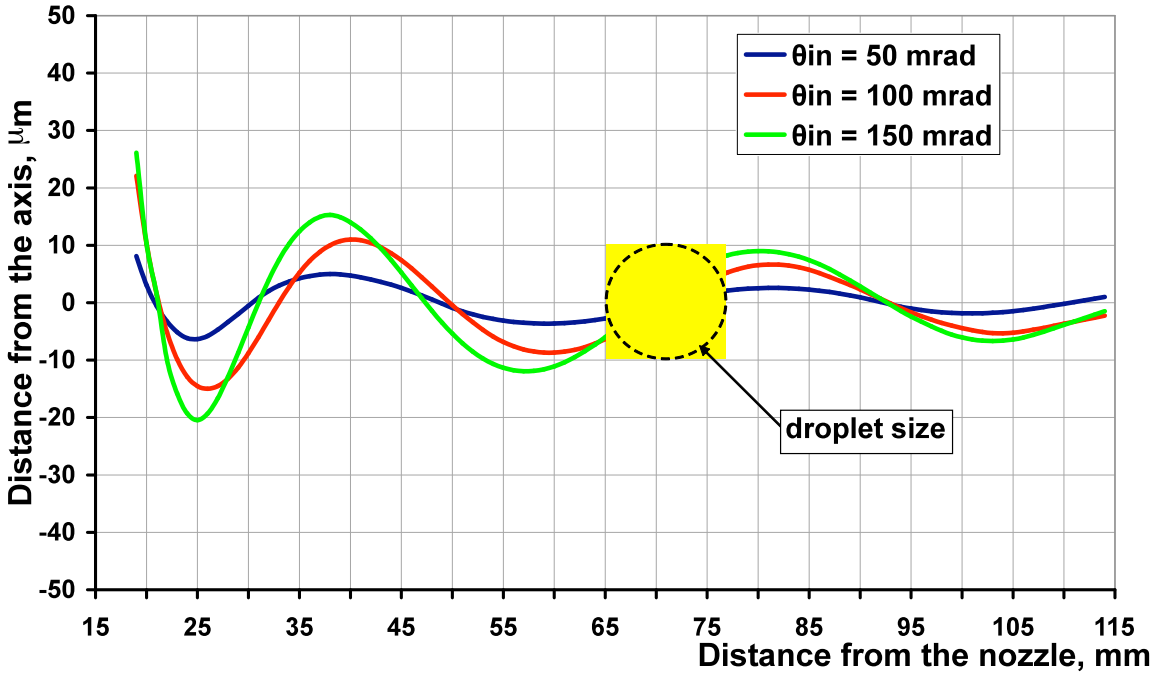

Fig.26. A more detailed view of the droplet trajectories shown in the Fig. 14. A droplet size is shown as a yellow circle for illustration.

5. DISCUSSION AND CONCLUSIONS

First of all I should note that there is a disagreement between value of final pellets velocity in my calculations and that one declared by Moscow-Jülich team (e.g. Refs. [18, 19]). So, in my simulations for the present Moscow-Jülich sluice and pellet diameter of 30 μm the final velocity V_{fin} = 191 m/s (see Fig. 13), but in the experiments of the Moscow-Jülich team the average velocity of 30 μm pellets amounts to ~70 m/s. One might say that there are some rough mistakes in my calculations, which is account for this disagreement. But I cannot agree with it because of:

first, results of my previous similar simulations [20], which I have performed for the buffer gas conditions and the sluice (or a "vacuum injection capillary") geometry of the Uppsala pellet-generator are in agreement with the measurements, in which a typical final velocity values range from 60 m/s to 100m/s [3],

second, the final pellet velocities in Moscow-Jülich pellet target, as a matter of principle and irrespective of results of my simulations, should be higher than that ones in the Uppsala pellet target because of the drag force $\mathbf{F}_D$ (1) inside the vacuum injection capillary of the Uppsala pellet-generator by a factor of five less than the drag force inside the present Moscow-Jülich sluice.

By means of detailed computer simulations it has been shown that to improve the performance of the Moscow-Jülich pellet target, it will be enough to make described above changes in the design of the 1st sluice and replace the 2nd sluice by the skimmer placed on the supersonic buffer gas axis upstream the Mach disk.
It will allow reduce required pumping speed of vacuum pumps by factor of 3.65 (from 602 l/s to 165 l/s).

An inter-droplet (and pellet) distance **L** is determined from $\mathbf{V_p = L \cdot f}$, where $\mathbf{V_p}$ is a droplet (or pellet) velocity and **f** is a frequency of a piezo-electric transducer. It means that for a given frequency **f** and for a given pellet diameter an effective pellet target thickness is inversely proportional to the final pellet velocity V_{fin}. So, the new sluice geometry has an

advantage over the present one since it provides for the pellet beam with lower pellets velocities (see Fig. 13 and Fig. 24).

On the other hand, a minimal inter-droplet distance cannot be less than the droplet diameter. As a result, it means that a maximum operational driving transducer frequency **f** is determined by a minimal droplets velocity that is achieved in droplet deceleration process in front of the sluice entrance. From this point of view the new sluice again has an advantage over the present one because the minimal droplets velocity here is 1 m/s compared to 0.35 m/s as it is in the case of present Moscow-Jülich sluice (see Fig.12 and Fig. 23).

The buffer gas flow conditions in vicinity of the nozzle exit has a strong impact on of the liquid jet formation and then its disintegration into droplets, but these processes are outside the scope of my computer simulations. Nevertheless, it is clear that the buffer gas flow conditions in this area are identical for the both sluices, which I explored in this work by means of computer experiments (the present Moscow-Jülich sluice and the new one). Therefore, I can assert that process of the liquid jet decay into droplets in the case of using the new sluice will take place in exactly the same way as it is in the present Moscow-Jülich pellet-generator.

In conclusion I should say that the suggested here new design of the 1st sluice cannot be considered as an optimal solution for an improvement of the Moscow-Jülich pellet-generator performance. Mainly, this report is a demonstration of powerful tools, which can be used for a further development of the PANDA pellet target by means of computer investigations.

Acknowledgements

I gratefully acknowledge fruitful and inspiring discussions with Markus Buscher, Hans Calen, Alfons Khoukaz, Inti Lehmann, Herbert Orth, Günther Rosner and Alexander Vasiliev. I thank Aleksandr Boukharov for information about the Moscow-Jülich pellet-generator design.

References

1. FAIR Baseline Technical Report, vol. 3B, 37 (2006).
2. O. Nordhage, Z.-K. Li, C.-J. Friden, G. Norman, U. Widner, Nucl. Instrum. and Meth. **A 546**, 391 (2005).
3. O. Nordhage, Ph.D. thesis, Acta Universitatis Upsaliensis, 2006, http://publications.uu.se/adstract.xsql?dbid=7137.
4. A. V. Boukharov, M. Buscher, A. S. Gerasimov, V. D. Chernetsky, P. V. Fedorets, I. N. Maryshev, A. A. Semenov, A. F. Ginevskii, Phys. Rev. Let., **100**, 174505 (2008).
5. A. V. Boukharov, private communication from 08.12.2008.
6. V. L. Varentsov, A. A. Ignatiev, Nucl. Instrum. and Meth. **A 413**, 447 (1998)
7. S. Schwarz, G. Bollen, D. Lawton, P. Loffy, D. J. Morrissey, J. Ottarson, R. Ringle, P. Schury, T. Sun, V. Varentsov, L. Weissman, Nucl. Instrum. and Meth. **B 204**, 507 (2003).
8. J. B. Neumayr, L. Beck, D. Habs, S. Heinz, J.Szerypo, P. G. Thirolf, V. Varentsov, F. Voit, D. Ackermann, M. Block, Z.Di, S.A. Eliseev, H. Geissel, F,Herfurth, F. P. Hessberger, S. Hofmann, H.-J. Kluge, S. Rahaman, C. Rauth, D. Rodriguez, C. Sheidenberger, G, Sikler, Z. Wang, C. Weber, W. R. Plass, M. Breitenfeldt, A. Chaudhuri, G. Marx, L. Shweikhard, A. F. Dodonov, Y. Novikov, M. Suhonen, Nucl. Instrum. and Meth. **B244**, 489 (2006).
9. V.L. Varentsov, N. Kuroda, Y. Nagata, H. A. Torii, M. Shibata, Y. Yamazaki, "*ASACUSA Gas-Jet Target: Present Status and Future Development",* Proc. of the Workshop on Physics with Ultra Slow Antiproton Beams, RIKEN, March 14-16, 2005, AIP Conf. Proc., **793**, 328 (2005).
10. V. L. Varentsov, D. Habs, Nucl. Instrum. and Meth. **A 490**, 16 (2002).
11. V. L. Varentsov, D. Habs, Nucl. Instrum. and Meth. **A 496**, 286 (2003).
12. Victor Varentsov, Michiharu Wada, Nucl. Instrum. and Meth. **A 532**, 210 (2004).
13. INTAS-GSI Research project, Ref. Nr 06-1000012-8956.
14. V. L. Varentsov, Int. Conf. on Micro- and Nanoelectronics 2007, Proc. SPIE, **Vol. 7025**, 702509 (2008); DOI:10.1117/12.802356.
15. V. L. Varentsov, 2008, unpublished.

16. J. Yang, R. Jaenicke, V. Dreiling, T. Peter, L. Aerosol Sci., **31**, 773 (2000).
17. http://www.beamdynamicsinc.com/
18. Minutes of JRA7/I3HP Pellet Target Meeting, 6 April 2006, IKP FZ-Jülich
19. Markus Buscher, "Moscow-Jülich pellet target", talk at PANDA Collaboration Meeting, Dubna, 04.07.2007.
20. V. L. Varentsov, "A new approach to the pellet-target generator design – variant 2", talk at PANDA TDR Target Meeting, Münster, 15.10.2008.